Multiple causes of ground deformation in the Napoli metropolitan area (Italy) from integrated Persistent Scatterers DinSAR, geological, hydrological, and urban infrastructure data

C. Terranova, G. Ventura, G. Vilardo

PII: S0012-8252(15)00061-6
DOI: doi: 10.1016/j.earscirev.2015.04.001
Reference: EARTH 2102

To appear in: *Earth Science Reviews*

Received date: 28 October 2014
Accepted date: 3 April 2015

Please cite this article as: Terranova, C., Ventura, G., Vilardo, G., Multiple causes of ground deformation in the Napoli metropolitan area (Italy) from integrated Persistent Scatterers DinSAR, geological, hydrological, and urban infrastructure data, *Earth Science Reviews* (2015), doi: 10.1016/j.earscirev.2015.04.001

Multiple causes of ground deformation in the Napoli metropolitan area (Italy) from integrated Persistent Scatterers DinSAR, geological, hydrological, and urban infrastructure data

C. Terranova[1], G. Ventura[2,3*], G. Vilardo[1]

[1] Istituto Nazionale di Geofisica e Vulcanologia, Osservatorio Vesuviano, Via Diocleziano 328, 80124 Napoli, Italy
[2] Istituto Nazionale di Geofisica e Vulcanologia, Via di Vigna Murata 605, 00143 Roma, Italy
[3] Istituto Ambeinte Marino Costiero, Consiglio Nazionale delle Ricerche, Calata Porta di Massa, interno Porto di Napoli 80, 80133 Napoli, Italy

*Corresponding author: Guido Ventura, Istituto Nazionale di Geofisica e Vulcanologia, Via di Vigna Murata 605, 00143 Roma, Italy, Phone +39 06 51860221; email: guido.ventura@ingv.it

Abstract

This study presents a Differential SAR Interferometry (DinSAR) interferometry analysis and review of ERS (1992-2001) and Radarsat (2003-2007) data on the city of Napoli (Italy). These data are processed using the Persistent Scatterers Interferometric synthetic aperture radar (PSinSAR) technique and post-processed by statistical selection and filtering with the aim to obtain, by combining ascending and descending geometry, the spatial distribution of the vertical and horizontal (east-west) components of the ground displacement velocity. We identify five main areas of subsidence affecting residential districts and strategic infrastructures (transportations and industrial plants). These are: a) Vomero-Arenella district; b) Scudillo-Stella district, c) Municipio Square; d) Garibaldi Square; e) Poggioreale district. In these areas, the ground deformation rate is between -1.3 and -10.5 mm/yr and varies through time. In particular, in the investigated time period, the subsidence rate (i) persistently increases in the Scudillo-Stella and Poggioreale districts, (ii) abruptly increases in

correspondence of underground construction activities (Municipo and Garibaldi squares), and (iii) decreases following the ground deformation style of the Campi Flegrei caldera (Vomero-Arenella district). More restricted areas of subsidence also occur in the northeastern, less urbanized, sectors of the Napoli metropolitan area. The subsidence triggering factors are investigated through a review of the available geological geomorphological, hydrological, and urban network information. With respect to other urban contexts, where the cause of subsidence is of natural or anthropogenic origin, Napoli shows a multiple association of triggering factors. These factors are: sub-soil excavations for the construction of transport infrastructures, filling/emptying cycles of large underground water reservoirs, gravity instability related to local morphological factors, raise of the water table with consequent hydrocompaction due to the stop of ground water withdrawal, and re-activation of volcano-tectonic faults associated to the uplift and subsidence phases (bradyseism) of the neighboring, active Campi Flegrei caldera, whose western sector includes a part of the Napoli urban area. We conclude that in a complex urban and geological setting like that of Napoli, ground deformations induced by anthropic and natural processes may coexist and should be monitored for a correct evaluation of the associated hazard and the management of the city planning activities. Finally, the combined review of satellite and geological data available for different urban districts worldwide is essential to identify the sources of ground deformation and analyze the time evolution of the related anthropic and/or natural processes.

Keywords: PSInSAR; DinSAR, Subsidence; Caldera dynamics; Water exploitation and use; Underground excavation; Monitoring; City planning; Hazard;

1. Introduction

The applications of differential radar interferometry for the observation and monitoring of ground deformation have increased due to the development, in the last decade, of the persistent (or permanent) scatterers (PS) technique (Colesanti et al., 2003; Crosetto et al., 2003; Ferretti et al., 2004, 2006). This technique, also known as point-target DinSAR, allows us to detect the line of sight (LOS) movements of man-made objects or natural reflectors characterized by radar coherence over time. Urban elements such as buildings, bridges, industrial plants, docks and piers are proper targets for differential radar interferometry applications. Land use changes due to urbanization have become one of the primary factors responsible for the subsidence in urban areas (Chen et al., 2012). In these areas, the subsidence has been ascribed to different causes including variations of the groundwater level (Lu and Liao, 2008; Liu et al., 2008; Zhang et al., 2011;), underground excavations (Fruneau et al., 2000; Tesauro et al., 2000; Wang et al., 2011), water drainage (Buckley et al. 2003; Engelkemeir et al., 2010; Yan et al., 2010; Hay-Man Ng et al., 2012), overloading of soil foundation and/or structural adjustment (Ding et al., 2004), compaction of fine sediments and/or organic-rich soils (Stramondo et al., 2008; Heleno et al., 2011), active tectonics and volcano dynamics (Vilardo et al., 2009, 2010), landslide and deep-seated gravitational deformations (Ventura et al., 2011). In spite of the large number of the possible causes of subsidence, most of the available studies based on satellite observations in urban areas analyze, with few exceptions (e.g., Ferretti et al., 2004, Lanari et al., 2004a; Kim et al., 2007; Terranova et al., 2012; Chaussard et al., 2014;), single sources of deformation.

Here, we study the deformation velocity field affecting the urban area of Napoli city (about 1 million inhabitants) because of (a) its urban network is affected by poorly known subsidence phenomena, and (b) the western sector of the urbanized area is partly located

within the dynamically active Campi Flegrei caldera. We perform a deformation analysis by using the multi-temporal (1992-2007) and multi-platform (ERS and Radarsat satellite missions) PSinSAR dataset from the TELLUS Project (Terranova et al., 2009). This dataset has been post-processed by Vilardo et al. (2009, 2010), who focused on (a) the large scale regional deformation of the Campanian region, and (b) the local scale intracaldera deformation of Campi Flegrei (Fig. 1). The same post-processing approach at a high spatial resolution is applied in this study on the city of Napoli. The obtained results are merged with the available geological and hydrological data, as well as the technical data concerning the urban configuration and infrastructure (i.e., underground galleries and stations, bridges, water reservoirs), and previous studies on the subsidence in limited areas. The joint interpretation and review of these data allow us to identify the causes of deformation and provide a comprehensive framework of the complex interaction between natural and anthropogenic factors, which could represent a major, underestimated geological hazard for the Napoli metropolitan area. Ultimately, we show how the review of merged satellite and geological information, which are available for many urban districts worldwide, allow us to reconstruct the time evolution of the ground deformations in densely populated areas and identify urban sectors where future satellite monitoring activities (e.g. ESA Sentinel-1 mission) should be implemented.

2. Geological setting, recent urban development, and deformations in the Napoli urban area

The Napoli metropolitan area is located within the Campanian Plain, a NW-SE elongated, Plio-Quaternary structural depression including the active volcanoes of Campi Flegrei (last eruption in 1538 AD) and Somma-Vesuvius (last eruption in 1944 AD) (Fig. 1a). The Campanian Plain is filled by an up to 4000 m thick sequence of Plio-Quaternary volcanic,

continental and marine deposits (Bruno et al., 2003; Piochi et al., 2005). Most of the volcanic deposits are affected by syn-eruptive and post-depositional alteration that produced lithified to semi-lithified tuffs and loose pyroclastic material know as ‘pozzolana’ (de' Gennaro et al., 1999; 2000). Unlithified, loose deposits consist of pumice lapilli and ash interstratified with paleosoils. The city of Napoli partly lies within the Campi Flegrei nested caldera, which formed subsequently to the Campanian Ignimbrite (CI; 39 ka) and Neapolitan Yellow Tuff (NYT; 15 ka) eruptions (Orsi et al., 1996; Scarpati et al., 1993, 2013). The western periphery of Napoli overlaps the CI caldera rim, and it is located inside the still active eastern sector of the NYT caldera (Cole et al., 2004; Perrotta et al., 2006; Sbrana et al., 2007; Scarpati et al., 2013) (Fig. 1a). The Napoli eastern periphery is within the Sebeto valley, which is located at the base of the northwestern flank of the Somma-Vesuvius volcano.

The lithologies of Napoli are characterized by a predominance of pyroclastic rocks (tuffs) mainly produced by the volcanic eruptions of phlegraean and neapolitan origin (Scarpati et al., 2013), and, subordinately, of Somma-Vesuvius (Fig. 1b) (Scarpati et al. 1993; Orsi et al., 1996). The hilly morphology of Napoli is mainly due to the presence of local monogenetic volcanoes (Scarpati et al., 2013). Few lavas were encountered in tunnel shallow excavations in the Vomero-Arenella district. Alluvial deposits and marine sediments, as well as anthropogenic land filling, predominate in the flat areas located along the present coastline and in the northern and western sectors of the city (Fig. 1b).

Thick CI and NYT deposits overlain older tuffs (Ancient Tuffs, AT) exposed along the scarps south of the Vomero-Arenella hill (Fig. 1b) (Perrotta et al., 2006; Scarpati et al., 2013). The Somma-Vesuvius tuffs are present in the subsurface of the eastern urban area (Corniello et al., 2002, 2003). The NYT yellowish and lithified tuff was commonly used as building material and many artificial scarps inside the city represent walls of abandoned quarries. These deposits are also incised by deep valleys later filled by reworked pyroclastic material

(Caliro et al., 1997). The NYT deposits are covered by a laterally discontinuous sequence of sandy silt and fine sands, gravels (pumice and scoriae layers), peats, anthropogenic sediments, and sea sandy deposits with alternated pumice and scoria beds, and fine to coarse ash levels (Comune di Napoli, 1967, 1999). The maximum thickness of this sequence is 20 m in the Vomero-Arenella area.

From a geotechnical perspective, the different rock types of Napoli show variable properties (Pellegrino et al., 1967; Baldi and Miraglino, 1999). For instance, the lithified NYT has an average value of the uniaxial compressive strength of 5 MPa and it is often affected by sub-vertical fractures (Tangenziale di Napoli, 2001). The unlithified facies of NYT has an internal friction angle of 30° to 38° and cohesion of about 0.02 MPa. (Pellegrino et al., 1967). However, in water saturation conditions, the cohesion is zero. The pumice layers and the volcanic and marine sands are cohesionless because of high permeability and porosity. The paleosoils and the urban landfill deposits represent the worst terrains in terms of geotechnical properties because of they have low compressive uniaxial strength and cohesion.

Until the early 1900s, in order to reduce the cost of the construction of new buildings in the city of Napoli, the pyroclastic deposits were widely exploited in the subsoil digging vertical pits of about 8-10 meters in the softer rocks. On the basis of the 1999 surveyed data, the Napoli Municipality estimated about 650.000 m^2 of caves, aqueducts and underground quarries affecting the basement of the urban area (Fig. 1b). After World War II, the large urban expansion has led to the creation of many new built up areas and associated underground services in the city centre and neighboring areas (Cantone, 2008). Consequently, many buildings have been constructed for decades over cavities, cisterns, parts of aqueducts and underground quarries. Sudden local collapses of buildings and rapid appearance of sinkholes are common phenomena and their genesis is often attributed to the presence of unstable underground cavities and/or loss of water from the aqueduct networks or from

sewers (Vallario, 1992). The widespread presence of ancient, buried buildings in the basement, the existence of three different underground aqueducts carried out on various levels during Greek, Roman and viceregal ages, and the presence of a large number of subterranean quarries, create additional severe geotechnical discontinuities in the soil foundations (Comune di Napoli, 1967).

From the hydrogeological point of view, the Napoli area may be divided into three sectors (Fig. 1b): western Campi Flegrei sector, central floodplain sectors and eastern Somma-Vesuvius sector (Celico et al, 2001; Corniello and Ducci, 2002, 2013). Bicarbonate-alkaline waters characterize the western sector, while bicarbonate and calcium-rich waters characterize the other two sectors (Celico et al., 1998). Also, the hydraulic gradient (i) in the western sector, which is $0.2\% < i < 0.8\%$, is higher than that of the central and eastern sectors ($i < 0.3\%$). This difference is due to the lower transmissivity T of the pyroclastics of the Campi Flegrei caldera ($10^{-2} < T < 10^{-4}$ m^2/s) with respect to that of the reworked alluvial deposits of the other two sectors, where $10^{-1} < T < 10^{-3}$ m^2/s. The NYT deposits show the lowest value of T ($10^{-5} < T < 10^{-5}$ m^2/s). The circulation of groundwater mainly develops by filtration into cracks and fractures for tuffs and lavas, and into pores for loose pyroclastics, marine sands and alluvial terrains. In the western and central hydrological sectors, which are characterized by morphological reliefs, the depth of the water table is lower with respect to that of the eastern sector, where the hydraulic circulation is strictly connected to that of the eastern Campanian Plain (Fig. 1a,b).

The Napoli aquifers were extensively exploited after World War II for industrial purposes and irrigation. This overexploitation of groundwater causes, in the eastern sector of Napoli, the drying up of shallow aquifers and some springs. The progressive abandonment, started in 1990, of the use of water for industrial, agricultural and domestic uses produced a

sudden increase of the groundwater level in the whole eastern area of Napoli, with the activation of many, previously unknown springs (Corniello and Ducci, 2003).

Results from leveling data (Del Gaudio et al., 2009), geological investigations (Di Vito et al., 1999; Cinque et al., 2011), and satellite studies on Napoli (Tesauro et al., 2000; Bonano et al., 2013; Lanari et al., 2004b; Vilardo et al., 2009 and 2010; Terranova et al., 2012) evidence that the urban area and its surroundings are affected by significant deformations. In the western sector of the Napoli urban area, minor uplift and subsidence episodes occurred in correspondence of the volcanic deformation events affecting the neighbor Campi Flegrei caldera (Lanari et al., 2004b; Vilardo et al., 2010; Terranova et al., 2012). Subsidences possibly correlated to the construction of the subway line and stations have been also detected in the central sector of the city (Tesauro et al., 2000; Bonano et l., 2013), while evidences of significant movements related to landslides or other gravity-related processes are lacking (Vilardo et al., 2009). Some subsidence areas located in the northeastern, less urbanized, sector of the city were also detected (Terranova et al., 2012). These latter are probably related to soil compaction and/or structural adjustment of constructions.

3. PSInSAR data review and post processing

In this study, we use two different radar data sets with ascending and descending observing geometry: the first one relates to ERS-1 and -2 (1992-2001), and the second one to Radarsat-1 (2003-2007). Both datasets have been interferometrically processed by means of the PSinSAR™ (Permanent Scatterers Interferometric synthetic aperture radar) analysis technique performed by the T.R.E. s.r.l. in the framework of TELLUS project (Terranova et al. 2009). The technique uses multiple radar images acquired from slightly different positions

comparing (or interfering) the different phases of the radar signal. The distance between the position of satellites at the time of the acquisition, in the plane perpendicular to the direction of orbit, is defined interferometric baseline (Curlander, 1982 and 1984). Shorter distances between the passes of the satellite (baseline) lower the dependency of the measurement by the topography of the area. In that case, the variation of the measured radar phase depends almost exclusively by the movement of the ground. In the radar data set used by us, we selected baselines lower than a critical value, which, for the ERS platform, is 937 m, corresponding to a distance between each satellite pass of tens or hundreds meters. The PSinSAR processing procedure (Ferretti et al., 2000, 2001; Colesanti et al., 2006) bases on the identification of permanent scatterers (PS), which are man-made objects (statues, heating and ventilating structures on the roofs of buildings, utility poles, dams, etc.) or natural (rock outcrops) reflectors characterized by stable individual radar-bright and radar-phase over long temporal series of interferometric SAR images. The phase data from PS are used to detect topographic changes which are expressed in terms of one-dimensional measurement of change in distance along the look direction of the radar spacecraft (line of sight; LOS).

The results of the PSinSAR™ processing, which also concerns the estimate and removal of the different contributions due to atmospheric anomaly, topographic effects and orbital ramps (Ferretti et al., 2000, 2004, 2006; Lu et al., 2008), consist of the time series of the sensor-target distance variations during ERS and Radarsat acquisition periods for ascending and descending satellite orbits. The precision on single PS LOS measurements depends on both the number of available SAR images and the PS multi-interferogram coherence. The SAR images used in this study allowed the accurate measurement of the PS movements along the SAR LOS. We select PS with a coherence > 0.65, which implies a millimetric accuracy (Colesanti et al., 2003; Ferretti et al., 2006; Lu et al., 2007). The PS yearly average displacement velocities in the LOS are calculated by linear fit of the variation

in distance between the target and the radar antenna. The final result is a measurement of the PS annual mean velocities within 1.0 mm/yr of accuracy (Fig. 2) (Ferretti et al., 2007; Colesanti et al., 2003; Vilardo et al., 2009, 2010).

The mean displacement rates are used to derive the average ground deformation velocity (mm/yr) maps in SAR coordinates for ascending and descending orbits of both ERS and Radarsat data by the inverse distance interpolation weighted method (IDW; Shepard, 1968). The radar LOS mean displacement velocity maps computed from the ascending and descending orbits, are successively combined to retrieve vertical and East-West mean displacement velocity maps of both ERS and Radarsat data (Lanari et al., 2004a,b; Lundgren et al., 2004; Manzo et al., 2006; Vilardo et al., 2009, 2010).

Before performing SAR data interpolation, with the aim to identify unstable larger urban districts and remove isolated deformations due to very local phenomena like the instability of a single building, isolated PS with the highest rate are removed after checking the location and nature of the scattering point. The filtering is performed interactively using the PS in both ascending and descending geometry superimposed on digital orthophotos and technical vector maps at 1:5000 scale. The next processing step concerned the estimate of the average ground deformation velocity maps over the entire time interval in radar LOS for ascending and descending orbits of both ERS and Radarsat data. This has been performed by IDW of each dataset using a quadratic weighting power 2 algorithm within a 500 m radius neighborhood to obtain a 5 m spaced grid. The IDW has been already applied to scattered set of satellite data by Inggs and Lord (1996), Girard and Girard (2003), Dermanis and Kostakis (2006), and Vilardo et al. (2009, 2010). In this interpolation method, a neighborhood about the interpolated point is identified and a weighted average is taken of the observation values within this neighborhood. The weights are a decreasing function of distance and the

neighborhood size is specified in terms of its radius (Shepard, 1968; Franke and Nielson, 1980).

By assuming that the ascending and descending radar LOS directions belong to the East-Z plane and the look-angle is the same for both ascending and descending geometries, the vertical and East-West displacement components have been retrieved by properly combining the radar LOS mean displacement velocity maps, computed from the ascending and descending orbits (Lanari et al., 2004a,b; Lundgren et al., 2004; Manzo et al., 2006; Vilardo et al., 2009, 2010). The results are shown in Fig. 3. The validation of the deformation trends recognized by PS-InSAR was already performed by Vilardo et al. (2009, 2010) comparing the mean vertical deformation velocities estimated from the ERS and Radarsat data with the corresponding velocity values recorded by the continuous GPS stations operating in the Campi Flegrei area. In order to check whether the investigated subsidence phenomena fit a linear model, LOS deformation time series for different sets of selected PS have been extracted from the data set of Vilardo et al. (2009) by following the procedure described in Vilardo et al. (2010). LOS time series are here presented for each of the investigated areas by selecting (a) the 20 PS with a maximum in the deformation rate over an extended (> 1 km^2) area (e.g. quarter or district; Figs. 4, 6, 12), or (b) all the PS located in a restricted area (e.g. square, subway station; Figs. 9 and 10). The LOS time series allow us to highlight the linear component of displacements and to determine the average value of the deformation rate of the selected PS.

4. Results and discussion

The analysis of the vertical component velocity maps allow us to identify several subsiding areas located within and outside the Napoli administrative boundaries (Fig. 3). In

general, the ERS data set (1992-2001) show a large subsidence in the Campi Flegrei caldera and more localized areas of subsidence within the Napoli urban area. The Flegrei subsidence is associated with a westward velocity trend, which is consistent with a deflation of the caldera (Vilardo et al., 2010). The Radarsat data set (2003-2007) records the uplift of the Campi Flegrei caldera due to bradyseismic activity (Orsi et al., 1996) and the associated eastward velocity trend affecting the caldera, and, to a lesser amount, the whole Napoli urban area (Vilardo et al., 2010).

Here, we investigate the areas of subsidence located within the central sector of the Napoli urban area, for which hydrogeological and geological data are available. We do not discuss the more restricted subsidences located in the less urbanized northeastern boundary of the Napoli metropolitan area (Fig. 3a) because of data are lacking and do not permit to draw reliable interpretations. For these subsidences, as previously reported, Terranova et al. (2012) suggest (a) possible compaction processes due to water table fluctuation, and (b) structural adjustment of urban infrastructures (e.g. highway overpasses, railway embankments, large foundation pillars). However, more data are necessary to unequivocally determine the factors responsible for these ground deformations.

Within this Napoli central sector, the vertical component evidences five main areas of deformation, whereas the E-W component maps show homogeneous velocity variations on the whole central sector of the city with the exception of the Scudillo-Stella district (Fig. 3b, d), whose horizontal component of deformation is discussed in Section 4.2. Taking into account general considerations summarized above, we focus the discussion on the vertical velocity patterns.

The subsidence areas recognized in Fig. 3 within the Napoli central sector include the urban zones named: a) Vomero-Arenella district (VA); b) Scudillo-Stella district (SS), c) Municipio Square (MS); d) Garibaldi Square (GS); e) Poggioreale district (PD). Table 1

summarizes the maximum deformation velocity for the 1992-2001 and 2003-2007 time periods in each of the above identified sectors. The maximum value of subsidence (up to -10.5 mm/yr) of the Napoli metropolitan area characterizes the Garibaldi Square. An increment of subsidence through time characterizes the Scudillo-Stella district, the Municipio and Garibaldi squares and the Poggioreale district. In Municipio and Garibaldi squares, significant subsidence phenomena appears after 2003. In the Vomero-Arenella district, the subsidence slightly decreases through time. With the exception of the Scudillo-Stella district, the other detected ground deformation areas have no a spatial relationship with the networks of artificial underground cavities of Napoli (see Figs. 1b and 3).

In the following, we illustrate the main geological, hydrological, and urban features of the five subsiding urban sectors of Napoli, and provide an interpretation of the causes of ground deformation. The geological, hydrological, and urban data we use are: a photogrammetric Digital Terrain Model 5 meter resolution (Regione Campania, SIT at http://sit.regione.campania.it/portal/portal/default/Home), the geotechnical and geolithological maps of Napoli (1:4000 and 1:10.000 scale, Comune di Napoli, 1999), the hydrogeological map of Napoli Province (1:50.000 scale; Provincia di Napoli Assessorato Miniere e Risorse Geotermiche, 2004), the network of subway tunnels and stations (1:18.000 scale; Comune di Napoli, 2004), the diagrams of sewage and underground water supply network (Comune di Napoli, 2004), the map of underground quarries, cavities and pits (1:20.000 scale; Comune di Napoli 2004), and the local subsurface geological information derived by exploration wells logs. These data are geo-referenced in UTM WGS84 coordinate system, organized in a GIS-based database, and integrated with the radar interferometry imagery. Data from technical reports and scientific publications on specific areas were also used. GIS was used to perform (a) a geospatial analysis of the different thematic layers with the aim to check, as an example, the relationships between the terrain slope and the horizontal component of the deformation

velocity, (b) the geostatistical analysis (interpolation) of the horizontal and vertical components of the deformation velocity, and (c) the overlap of different thematic maps, e.g., the hydrogeological map, the urban infrastructure map, and the satellite-derived deformation maps.

4.1 The Vomero-Arenella district

4.1.1 Geological and hydrological setting

The largest (about 1.5 km^2) ground deformation area of Napoli involves the Vomero-Arenella district. This area shows a persistence of the subsidence during the 1992-2001 and 2003-2007 time periods, but with decreasing velocity values through time (Fig. 4; Table 1). Tesauro et al. (2000) also detected a subsidence in this area in the 1993-1995 time period, and relate this deformation to the construction of the subway. The Vomero-Arenella district is a NE-SW slightly elongated morphological plateau with altitudes between 160 and 180 m a.s.l.. This plateau is bounded by the morphological scarps of the Campi Flegrei CI caldera faults (Fig. 4; Perrotta et al., 2006; Amato et al., 2009). The present morphology was shaped over the centuries by the extraction of tuffs and by subsequent filling of the excavation fronts and watercourses with landfill materials, and later by intense urbanization. According to Cole et al. (1994) and Scarpati et al. (2013), a dome-like lava body occurs at about 150 m depth below the Vomero-Arenella ground level. This body is covered by the pre-CI deposits, CI deposits and by an up to 80-100 m thick sequence of partly lithified NYT rocks. The uppermost, up to 20 m thick, sediments are pumices and ash layers of the post-NYT activity of Campi Flegrei (Scarpati et al., 2013). The water table is at a depth of about 10 m a.s.l., i.e., at a depth of 150-170 m from the Vomero-Arenella ground level (Allocca and Celico, 2008).

4.1.2 Causes of the ground deformation

The lack of significant, large cavities in the Vomero-Arenella substratum, the absence of correlations between deformation velocity and thickness of the shallower sediments, and, as previously reported, the occurrence of an aquifer at a depth of 150-170 m from the ground level exclude that the detected subsidence is associated with subsoil-related instability or to the dynamics of the water table. Also, we exclude that the subsidence can be fully ascribed to the construction of the subway, as suggested by Tesauro et al. (2000), because (a) the subsiding area has a surface of about 4 km^2; as also noted by these authors, '*the extension of the subsided area is quite large compared to what expected from the effect of soil volume loss due to the excavation works*' (Tesauro et al., 2000), (b) the subway track is below a part of the southern sector of the subsiding area, and does not crosses the northern and eastern sectors (see Figs. 1, 2 and 4, and figure 5 in Tesauro et al., 2000), and (c) the subsidence continues from 1992 to 2007, whereas the construction activities of the subway tunnel ended in 1995. As a result, the causes of Vomero-Arenella ground deformation must be likely sought in its geological structure. According to the results from leveling data collected between 2006 and 2008, Del Gaudio et al. (2009) show that the dynamics of the Vomero-Arenella area is strictly related to that of the NYT caldera. Our data indicate a subsidence rate of -5.6 mm/yr between 2003 and 2007, a value fully consistent with those estimated by Del Gaudio et al. (2009), which are between -2.5 and -5.0 mm/yr. The data of Fig. 5 indicate that two main areas of subsidence affect the Vomero-Arenella district: the first one is delimited by the CI caldera faults, and the other one is located in correspondence of the NYT caldera rim. Therefore, the recognized subsiding areas are confined by the CI and NYT caldera faults (Fig. 4a) (Perrotta et al. 2006, Amato et al., 2009; Cinque et al., 2011), which are part of a regional structure. In addition, the Vomero-Arenella area is located within the NYT caldera (Fig. 1). We propose that the Vomero-Arenella subsidence is controlled by the NYT and CI caldera faults. These

faults, which were also reactivated during the NYT collapse, are still active and possibly sensitive to the volcano dynamics of the Campi Flegrei caldera. In fact, the interferometric processing referred to the 2003-2007 period (Figs. 4b and 5) evidences an attenuation of subsidence during the uplifting phase of the central sector of the Campi Flegrei caldera. The deformation style of Vomero-Arenella district, i.e. subsidence along caldera faults bounding a single block, is consistent with the re-activation of the Campi Flegrei inner and bordering faults, which produce a block-like differential buckle (Orsi et al., 1996; Di Vito et al., 1999).

4.2 The Scudillo-Stella district

4.2.1 Geological, hydrological and urban setting

The Scudillo-Stella subsiding area represents the site of ground deformation inside the urban area of Napoli with peculiar characteristics of the subsidence rate and persistence of the movements (Figs. 3 and 6). This area is characterized by an increase of deformation velocity through time with maximum values of about -8.6 mm/yr (Fig. 6b; Table 1). The Scudillo-Stella district (average altitude of 220 m a.s.l.) is a low density built-up area characterized by a 3° to 15° dipping, southeast facing morphological bulge laterally bounded by incisions. The water table below Scudillo-Stella is at a depth of 14 to 18 m a.s.l. (Celico et al., 2001). Figure 7 shows the stratigraphy of wells located around the district (Comune di Napoli, 1999; Tangenziale di Napoli, 2001). The local stratigraphy reconstructed from these wells shows a 4 m thick succession of artificially reworked pyroclastic deposits and pumice levels with different degree of compaction below Scudillo. These reworked deposits represent the anthropic landfill of Scudillo. This succession covers 6 to 8 m thick yellow tuff cohesive deposits (NYT), whose thickness increases moving away from the subsiding area (Figs. 6 and 7). The yellow tuffs, which are affected by subvertical fractures, cover an up to 30 m thick

succession of gray ash including sandy layers with pumices and scorias. The geotechnical tests carried out on these latter deposits underlying the NYT reveal a cohesion approaching 0 (Tangenziale di Napoli, 2001).

A large, artificial network of cavities measuring about 350 x 150 x 10 m with a surface area of 5.25 x 10^4 m^2 occurs within the NYT deposits of Scudillo (Figs. 6, 7 and 8) (https://www.arin.na.it/index.php?id_page=27 https://www.arin.na.it/index.php?id_page=27). This cavity network is located at about 180 m a.s.l. (about 40 m below the average ground level) and it is currently used by the water distribution company of Napoli, which built (with additional concrete elements and waterproofing works) the larger drinking water reservoir of the city (estimated capacity of 145,000 m^3). Data collected by us in the galleries surrounding the main reservoir show that the NYT deposits are affected by 20 to 40 m spaced cracks with a prevailing NW-SE strike and a second-order NE-SW strike (inset of Fig. 6b).

4.2.2 Causes of the ground deformation

On the basis of the above reported data, we exclude that the Scudillo subsidence is triggered by (a) hydrological causes like variations in the water table depth, (b) faulting activity, and (c) soil softening because the water table is at a depth of 200 m from the ground level, active faults are lacking, and no relation exists between soil thickness and deformation velocity. In fact, the subsiding area is centered on the main cavity (Fig. 8), whose filling/emptying cycles (loading/unloading effect) may have damaged the NYT deposits, and the underlying cohesionless pyroclastics. The major evidence of damage of NYT is the occurrence of fractures in the galleries of the water distribution reservoir (Fig. 6b, inset). With the available elements, the deformation recorded on Scudillo could be due to the above reported artificial cause and, to a general gravity instability of the morphological bulge (slope

angle up to 15°; Fig. 8), as suggested by the up to 2 mm/yr eastward velocity component in the Radarsat map (Fig. 3b,d).

4.3 The Municipio Square and the Garibaldi Square

4.3.1 Geological, hydrological, and urban setting

Municipio Square is located in the seafront of the Napoli harbour (Fig. 1b); the square lies within an ancient, now disappeared, natural bay used as harbour until the V century A.D.. Later, the bay was filled and drained. The subsoil consists of sandy silt covering the NYT deposits, which have been found at 35 meters below the ground level (http://www.rocksoil.com/pdf/Metronapoli.pdf). In this area, the water table is at about 2 m below the ground (Amato et al., 2009).

Garibaldi Square is located in front of the Central railway station of Napoli (Fig. 1b) over a subsoil constituted by volcanic sand and silt deposits with intercalations of pumiceous lapilli covering the NYT deposits (Amato et al., 2009). The NYT deposits are at depth between 20 and 40 meters from the ground level. The construction of the Line 1 of the Napoli subway started in 2002 with geognostic drilling and drainage. Soil freezing activities started at the end of 2004, and the underground subway station excavation begun in June 2005. The excavations were carried out below the water table at about 30 meters of depth in Municipio, where the piezometric level of groundwater was about 1.5 meter below the ground level (http://www.rocksoil.com/pdf/Metronapoli.pdf). The subway gallery consists of two, 11 m spaced pipes with 5.8 meters of internal diameter; the underground stations have a rectangular, 20 x 45 m shape and are at a depth between 35 and 50 meters below the ground.

Subway galleries are built with a cap crossing the NYT deposits and the overlying sand. During the subway construction, the underground structures have been realized with the technique of soil freezing preceded by extensive groundwater pumping with the aim of reducing the hydraulic head (http://www.rocksoil.com/pdf/Metronapoli.pdf).

4.3.2 Causes of the ground deformation

The ground deformation anomalies detected in Municipio Square and Garibaldi Square during the 2003-2007 observing period result from the construction of the subway (Figs. 9 and 10). According to this interpretation, no ground deformations are detected in the ERS dataset (1992-2001), i.e. in the period preceding the excavation activities (Figs. 9a and 10a). Radarsat data (2003-2007; Figs. 9b and 10b) show comparable velocity trends and behavior for both PS on buildings and street floors, indicating an overall ground deformation. Bonanno et al. (2013) also detected a subsidence between 2003 and 2008 in two, selected PS located on the Napoli Railway Station, in front of the Garibaldi square. They record a small uplift (1 mm/yr) between January and May 2010. Bonanno et al. (2003) suggest that the subsidence is related to the subway tunnel construction below Garibaldi square. However, excavation activities in Garibaldi square started in 2005. Accordingly, the time series values of individual PS we have identified on buildings and ground point out that the subsidence started after the beginning of underground excavation activities (Fig. 11 and Table 1). On the basis of our data, we propose that (a) the subway excavation activities carried out from 2005, (b) the weight of the temporary and permanent underground structures, and (c) the intensive drainage of the groundwater and soil freezing before 2005 lead to the detected subsidence phenomena. In particular, an extensive and massive drainage of groundwater using pumping stations reduced the fine fraction from the sand and pyroclastic deposits promoting soil compaction phenomena (Cantone, 2008). The maximum subsidence rate deduced from the

analysis of the Radarsat LOS data in the Municipio Square between 2002 and 2005, when the drainage and soil freezing activities started, was of -1.5 mm/yr (Table 1). In the time period of the gallery construction, between 2005 and 2007, the subsidence was of -9.5 mm/yr (Table 1; Fig. 11). These values are consistent with the ground measurements from geotechnical monitoring carried out during the construction, which show a subsidence of -1.5 mm/yr between 2004 and 2005, and of -10 mm/yr between 2005 and 2006 (Cantone, 2008).

4.4 Poggioreale district

4.4.1 Geological, hydrological, and urban setting

Poggioreale is located in the eastern area of Napoli (Fig. 1b). The district developed on an alluvial plain on which the Central railway station and some industrial activities are located (orthophoto in Fig. 12). In this area, the subsoil deposits consist of reworked pyroclastics and limno-marsh and marine deposits with discontinuous lens of 5 to 10 m thick peats (Corniello and Ducci, 2002). Below these deposits, a 10 m thick, incoherent to lithified sequence of Somma-Vesuvius tuffs has been encountered at 20 m below the ground. These tuffs cover an up to 60 m thick succession characterized by metric levels of coarse sand alternating with dark fine sands, ashes and pumices. An artesian aquifer passes through the tuffs below the Poggioreale district (Allocca and Celico, 2008, 2009). In this sequence, the CI deposits are lacking (Bellucci et al., 1994). At Poggioreale, the rising of the ground water is a phenomenon developed in the last twenty years, when the activities of groundwater exploitation stopped (Corniello and Ducci, 2002) and the groundwater withdrawals significantly reduced from $3.1 \cdot 10^7$ m^3/yr in 1992 to $4.7 \cdot 10^6$ m^3/yr in 2001. In the subsiding Poggioreale area (Fig. 12), the rise of the water table from 2-3 m below the ground in 1992 to < 1 m in 2001 produced overflowing phenomena (Corniello and Ducci, 2013). Between 1992

and 2002, the subsidence rate was of -1.6 mm/yr (Table 1) and the average rise rate of the water table was of 0.5 m/yr (Fig. 12c). Between 2003 and 2007, the ground subsidence and raise rate of the water table increased to -7.8 mm/yr and 0.8 m/yr, respectively.

4.4.2 Causes of the ground deformation

The observed Poggioreale subsidence is associated to a rise of the water table. Such a rise should produce an uplift, however, the progressive wetting of soil may also produce hydrocompaction, a phenomenon observed in flat areas and volcanic terrains like those of Poggioreale (Amin and Bankher, 1997). According to Lofgren (1969), hydrocompaction processes, which also affect extensive areas in North America, Europe, and Asia, may develop in loose, dry, low-density deposits that compact when they are wetted. The compaction by wetting produces widespread subsidence of the land surface because the infiltrating water enters the pores of the sediment and weakens the interparticle bonds reducing the capillary tension between coarser soil particles that provided strength when unsaturated. Removal of these bonds causes overall consolidation (Stumf, 2013). The Poggioreale terrains include loose, reworked pyroclastics, limno-marsh deposits and incoherent tuffs with dark fine sand, ash and pumice. The density values are between 800 and 1400 kg/m^3, and the porosity between 52 and 57 % (Pellegrino et al., 1967). The available oedometer tests (Pellegrino et al., 1967) show that, when saturated, the terrain collapses at a constant pressure. After the collapse, the sample slightly deforms at increasing pressures. The strain is not recovered when the pressure is removed (Fig. 12 d). The above summarized data indicate that the Poggioreale terrains have the required characteristics for possible hydrocompaction by progressive wetting because they are incoherent, include a fine fraction (volcanic ash and a limnic component) and have a low density (pumices). The results of the

oedometer test are also consistent with those of collapsible soils by hydrocompaction (Mansour et al., 2008).

Based on the above summarized data and considerations, the subsidence of the Poggioreale district could be explained by a worsening of the technical characteristics of foundation soils due to hydrocompaction processes. These processes are related to the condition of water saturation that occurred after 1992. In addition, the higher values of subsidence detected by Radarsat data cluster on the main railway elements including the embankment (Fig. 12b), which, with respect to the surrounding industrial warehouses, represent structures with concentrated load. Other significant, spot-like subsidences occur in correspondence of an E-W trending flyover and abandoned industrial areas (Fig. 12). We remark that the ground subsidence detected by Radarsat data includes the depressed areas with the highest flood hazard due to the raise of the water table over the ground (Regione Campania, 2005).

5. Conclusions

Our study shows that five zones with extension up to 1.5 $km^2$of the Napoli urban area are affected by ground deformation (subsidence) with rates up to -10.5 mm/yr. These zones are: the Vomero-Arenella district and Scudillo-Stella district (western sector), Municipo and Garibaldi squares (central sector), and the Poggioreale district (eastern sector).

The causes of subsidence include volcanotectonic processes associated with the reactivation of the Campi Flegrei caldera bounding faults, loading/unloading cycles associated to the filling/emptying of water within a subterranean, large reservoir possibly associated to local gravity instability processes, activities for the construction of subway

transport infrastructures, and elevation of the water table due to reduction and of groundwater exploitation with consequent hydrocompaction.

Between 1992 and 2007, the subsidence rate is not constant and (a) persistently increases in the Scudillo-Stella and Poggioreale districts, (b) abruptly increases in correspondence of yard underground activities (Municipo and Garibaldi squares), and (c) decreases following the ground deformation style of the Campi Flegrei caldera (Vomero-Arenella district). On the basis of these results, a continuous monitoring of the subsidence must be implemented, mainly in the Scudillo Stella and Poggioreale districts, along with operational actions aimed to reduce the hazard related to potential, sudden accelerations of deformation. In addition, further studies are required to investigate the causes of subsidence in the areas located close to the eastern boundary of the Napoli municipality (Fig. 3).

In a more general context, deformations related to caldera dynamics like those of Napoli are observed at other cities, e.g. Kokubu (Aira caldera, Japan) (Remy et al., 2006), while the subsidence induced by use of groundwater also affect Paris (France; Fruneau et al., 2005), Mexico City (Mexico; Osmanoğlu et al., 2011), Houston (Texas; Buckley et al., 2003; Engelkemeir et al., 2010), Lisbon (Portugal; Heleno et al., 2011), and Los Angeles (California, Lanari et al., 2004a). As detected in the Municipo and Garibaldi squares of Napoli and other urban areas, e.g. Shangai (China; Wang et al., 2011), underground excavations may also play a role in triggering subsidence. However, the above cited examples concern ground deformations associated to a single, anthropic or natural cause. Our results on Napoli show that unrelated anthropic and natural sources of subsidence may coexist showing the complexity and the multidisciplinary character for city management.

Acknowledgements We thank Ing. G. Sorgenti by ABC water supply company for the permission to access the underground structures of the Scudillo area, Arch. F. Pignataro of

Napoli Municipality for providing ancillary thematic data used in this work, and Tangenziale di Napoli S.p.A. for the well logs and geotechnical data. We thank two anonymous reviewers and Claudio Scarpati for the perceptive comments and suggestions, which greatly improved the data presentation and interpretation. We also thank Shuhab Khan for the editorial handling and comments. G. Ventura was supported by the UNESCO - IYPE project 'Creep'.

References

Allocca, V., Celico, P., 2008. Scenari idrodinamici nella piana ad Oriente di Napoli (Italia) nell'ultimo secolo: cause e problematiche idrogeologiche connesse. Giorn. Geol. App., 9 (2), 175-198.

Allocca, V., Celico, P., 2009. Le risorse dell'acquifero vulcanico a Nord-Ovest del Somma-Vesuvio (Napoli): idrodinamica, qualità e quantità. In Calcaterra, D., Morra, V., (Eds.), Atti del Convegno Internazionale Montagne di Fuoco Napoli Nicolosi, 109-124.

Amato, L., Carsana, V.,Cinque, A., Di Donato, V.,Gianpaola, D., Guastaferro, C., Irollo, G., Morhange, C., Romano, P., Ruello, M. R., Ermolli, E., 2009. Evoluzione del paesaggio costiero tra Parthenope e Neapolis. Méditerranée, 112, 23-31.

Amin, A., Bankher, K., 1997. Causes of Land Subsidence in the Kingdom of Saudi Arabia. Natural Hazards, 16, 57-63, doi: 10.1023/A%3A1007942021332

Baldi, G., Miraglino, P., 1999. Relazione geologica alla variante del PRG di Napoli. Comune di Napoli Assessorato alla vivibilità, Servizio di Pianificazione Urbanistica, 108 pp.

Bellucci, F. 1998. Nuove conoscenze stratigrafiche sui depositi effusivi ed esplosivi nel sottosuolo dell'area del Somma-Vesuvio. Bollettino della Società Geologica Italiana, 117(2), 385-405.

Bonano, M., Manunta, M., Pepe, A., Paglia, L., Lanari, R., 2013. From Previous C-Band to New X-Band SAR Systems: Assessment of the DInSAR Mapping Improvement for Deformation Time-Series Retrieval in Urban Areas. Geoscience and Remote Sensing, IEEE Transactions, 51, 1973-1984, doi: 10.1109/TGRS.2012.2232933

Bruno, P. P. G., Rapolla, A., Di Fiore, V., 2003. Structural settings of the Bay of Naples (Italy) by seismic reflection data: Implications for the Campanian volcanism. Tectonophys, 372, 193–213.

Buckley, S.M., Rosen, P.A., Hensley, S., Tapley, B.D., 2003. Land subsidence in Houston, Texas, measured by radar interferometry and constrained by extensometers. J. Geophys. Res., 108(B11), 2542, doi:10.1029/2002JB001848.

Caliro, S., Franzese, G., Galateri, C., Galatei, G., Imperato, M., Milia, A., Monetti, V., Nardi G., Ortolani, F., Pagliuca, S., Putignano, M.L., Stanzione, D., Toccaceli, R., 1997. Area Urbana di Napoli: Principali caratteristiche geologiche stratigrafiche ed ambientali. Atti Convegno 'Geologia delle grandi aree urbane' Progetto Strategico CNR, Bologna, 120-144.

Cantone, A., 2008. Comportamento di scavi profondi in ambiente urbano. PhD thesis in Ingegneria geotecnica, Università degli studi di Napoli Federico II, www.fedoa.unina.it/8446/1/Cantone_Antonella_23.pdf

Celico, F., Esposito, L., Mancuso, M., 2001. Hydrodynamic and hydrochemical complexity of Napoli urban area: some interpretations. Geol. Tecn. Amb., 2, 35-54.

Celico, P., Stanzione, D., Esposito, L., Ghiara, M.R., Piscopo, V., Caliro, S., La Gioia, P., 1998. Caratterizzazione idrogeologica e idrogeochimica dell'area vesuviana. Boll. Soc. Geol. It., 117, 3-20.

Chatterjee, R.S., Fruneau, B., Rudant, J.P., Roy, P.S., Frison, P.L., Lakhera R.C., Dadhwal, V.K., Saha, R., 2006. Subsidence of Kolkata (Calcutta) City, India during the 1990s as observed from space by differential synthetic aperture radar interferometry (D-InSAR) technique. Remot. Sens. Env., 102 (1-2), 176-185.

Chaussard, E., Wdowinski, S., Cabral-Cano, E., Amelung, F., 2014. Land subsidence in central Mexico detected by ALOS InSAR time-series. Remot. Sens. Env., 140, 94-106, doi: 10.1016/j.rse.2013.08.038

Chen, F., Lin, H., Zhang, Y., Lu, Z., 2012. Ground subsidence geo-hazards induced by rapid urbanization: implications from InSAR observation and geological analysis. Nat. Haz. Earth Syst. Sci., 12, 935–942, doi:10.5194/nhess-12-935-2012.

Cinque, A., Irollo, G., Romano, P., Ruello, M.R., Amato, L., Giampaola, D., 2011. Ground movements and sea level changes in urban areas; 5000 years of geological and archaeological record from Naples southern Italy. Quater. Intern., 232, 1–2, 45–55, doi: 10.1016/j.quaint.2010.06.027.

Cole, P.D., Perrotta, A., Scarpati, C.,1994. The volcanic history of the southwestern part of the city of Naples. Geol. Magaz., 131, 785-799.

Colesanti, C., Ferretti, A., Prati, C., 2003. Monitoring landslides and tectonic motions with the permanent scatterers technique. Eng. Geol., 68 (1), 3-14.

Comune di Napoli (1967). Il sottosuolo di Napoli. I Commissione, Comune di Napoli, Napoli, 446 pp.

Comune di Napoli (1999). Indagini geologiche per l'adeguamento del PRG alla Legge Regionale 7-1-1983 n.9 in difesa del territorio sismico. Servizio Urbanistica, Commissario Ad Acta L.R. 9/83, 108 pp.

Comune di Napoli (2005). Variante generale al Piano Regolatore, deliberazione del Consiglio comunale n. 55 del 24 giugno 2005 (http://www.comune.napoli.it/flex/cm/pages/ServeBLOB.php/L/IT/IDPagina/2166).

Corniello, A., Ducci, D., 2002. Hazardous piezometric levels rising in Naples urban area (Italy) as a consequence of overexploitation reduction. Proceedings of SINEX Symposium of Intensive Use of Groundwater, Valencia (Spain), 10 pp.

Corniello, A., Ducci, D., 2013. Hydrogeological features. From groundwater problem to groundwater opportunity. In: Moccia, F., Palestino, M.F., (Eds.), Inhabiting the Future, Cleanedizionoi, Napoli, 106-118.

Corniello, A., Ducci, D., Catapano, O., Monti, G.M., 2003. Variazioni piezometriche nella zona orientale della città di Napoli. Quad. Geol. Appl., 101, 43-57.

Crosetto, M., Castillo, M., Arbiol, R., 2003. Urban subsidence monitoring using radar interferometry: Algorithms and validation. Photogram. Eng. Rem. Sens.., 69 (7), 775-783.

Curlander, J.C., 1982. Location of Spaceborne SAR Imagery. IEE Trans. Geosc. and Rem. Sens., 20, 359-364.

Curlander, J.C., 1984. Utilization of Spaceborne SAR Data for Mapping. IEE Trans. Geosc. and Rem. Sens., 22, 106-112.

de' Gennaro, M., Incoronato, A., Mastrolorenzo, G., Adabbo, M., Spina, G., 1999. Depositional mechanisms and alteration processes in different types of pyroclastic deposits from Campi Flegrei volcanic field (Southern Italy). J. Volcanol. Geotherm. Res., 91, 303-320.

Del Gaudio, C., Aquino, I., Ricco, C., Serio, C., 2008. Monitoraggio geodetico dell'area vulcanica napoletana: risultati della livellazione geometrica di precisione eseguita ai Campi Flegrei a settembre 2008. Quaderni di Geofisica, 66, 1-13 (http://istituto.ingv.it/l-ingv/produzione-scientifica/quaderni-di-geofisica/archivio/quaderni-di-geofisica-2009/).

Dermanis,A., Kotsakis, C., 2006. Estimating Crustal Deformation Parameters from Geodetic Data: Review of Existing Methodologies, Open Problems and New Challenges. In: Geodetic Deformation Monitoring: From Geophysical to Engineering Roles. Springer-Verlag, Berlin, IAGS, 131, 7-18.

Di Vito, M.A., Isaia, R., Orsi, G., Southon, J., de Vita, S., D'Antonio, M., Pappalardo, L., Piochi, M., 1999. Volcanism and deformation since 12,000 years at the Campi Flegrei caldera Italy. J. Volcanol. Geotherm. Res., 91, 221-246

Ding, X.L., Liu, G.X., Li, Z.W., Li, Z.L., Chen, Y.Q. ,2004. Ground subsidence monitoring in Hong Kong with satellite SAR interferometry. Photogram. Eng. Rem. Sens., 70 (10),1151-1156.

Engelkemeir, R., Khan, S.D., Burke, K., 2010. Surface deformation in Houston, Texas using GPS. Tectonophysics, 490 (1-2): 47-54, doi: 10.1016/j.tecto.2010.04.016

Ferretti, A., Prati, C., Rocca,, F., 2000. Nonlinear Subsidence Rate Estimation using Permanent Scatterers in Differential Interferometry. IEEE Trans. Geosci. Rem. Sens., 38 (5), 2202-2212.

Ferretti, A., Novali, F., Burgmann, R., Hilley, G., Prati, C., 2004. InSAR Permanent Scatterer Analysis Reveals Ups and Downs in San Francisco Bay Area. EOS, 85 (34), 1-3.

Ferretti, A., Prati, C., Rocca, F., Wasowski, J., 2006. Satellite interferometry for monitoring ground deformations in the urban environment. IAEG 2006, Geological Society of London, Nottingham, Paper 284.

Ferretti,A., Savio, G., Barzaghi, R., Borghi, A., Musazzi, S., Novali, F., Prati, C., Rocca, F., 2007. Submillimeter Accuracy of InSAR Time Series: Experimental Validation. IEEE Trans, Geosci. Remote Sensing, 45 (5), 1142–1153.

Franke, R., Nielson, G., 1980. Smooth interpolation of large sets of scattered data. Int. J. Numer. Meth. Eng., 15, 1691-1704, doi: 10.1002/nme.1620151110

Fruneau, B., Sarti, F., 2000. Detection of ground subsidence in the city of Paris using radar interferometry: isolation of deformation from atmospheric artifacts using correlation. Geophys. Res. Let, 27 (24), 3981-3984.

Fruneau, N., Deffontaines, B., Rudant, J.P., Le Parmentier, A.M., 2005. Monitoring vertical deformation due to water pumping in the city of Paris (France) with differential interferometry. Compt. Rend. Geosci., 337 (13), 1173-1183.

Girard, C.M., Girard M. (2003). Processing of Remote Sensing Data. CRC Press-Taylor & Francis, London, 508 pp.

Hay-Man Ng, A., Ge, L., Li, X., Zhang, K., 2012. Monitoring ground deformation in Beijing, China with persistent scatterer SAR interferometry. J. Geod., 86, 375–392, doi: 10.1007/s00190-011-0525-4

Heleno, S.I.N., Oliveira, L.G.S., Henriques, M.J., Falcão, A.P., Lima, J.N.P., Cooksley, G., Ferretti, A., Fonseca, A.M., Lobo-Ferreira, J.P., Fonseca, J.F., 2011. Persistent Scatterers Interferometry detects and measures ground subsidence in Lisbon. Rem. Sens. Env., 115(8), 2152-2167, doi:10.1016/j.rse.2011.04.021 pp.2152-2167.

Hillel, D., 1998. Environmental Soil Physics: Fundamentals, Applications, and Environmental Considerations. Academic Press, London, 771 pp.

Kim, J., Kim, D., Kim, S., Won, J., Moon, W.M., 2007. Monitoring of urban land surface subsidence using PSInSAR. Geosci. J., 11 (1), 59 - 73.

Inggs, M.R., Lord, R.T., 1996. Interpolating Satellite Derived Wind Field Data Using Ordinary Kriging, with Application to the Nadir Gap. IEEE Trans. Geosc. and Rem. Sens., 34, 250-256.

Lanari, R., Lundgren, P., Manzo, M., Casi, F., 2004a. Satellite radar interferometry time series analysis of surface deformation for Los Angeles, California. Geophys. Res. Lett., 31, L23613, doi:10.1029/2004GL021294

Lanari, R., Berardino, P., Borgström, S., Del Gaudio, C., De Martino, P., Fornaro, G., 2004b. The use of IFSAR and classical geodetic techniques for caldera unrest episodes: application to the Campi Flegrei uplift event of 2000. J. Volcanol. Geotherm. Res., 133, 247−260.

Lofgren, B.E., 1969. Land subsidence due to the application of water. Rev. Eng. Geol., 2, 271-304.

Liu, G., Luo, X., Chen, Q., Huang, D., Ding, X., 2008. Detecting Land Subsidence in Shanghai by PS-Networking SAR. Interferom. Sens., 8, 4725-4741.

Lu, L., Liao, M., 2008. Subsidence measurements with PS-InSAR techniques in Shanghai basin. Int. Arch. Photogramm. Rem. Sens. Spat. Inf. Sci., XXXVII (Part B7), 173–178.

Lundgren, P., Casu, F., Manzo, M., Pepe, A., Berardino, P., Sansosti, E., 2004. Gravity and magma induced spreading of Mount Etna volcano revealed by satellite radar interferometry. Geophys. Res. Lett., 31, L04602. doi:10.1029/2003GL018736.

Mansour, Z.M., Chik, Z., Taha, M.R., 2008. On the Procedures of Soil Collapse Potential Evaluation. Journal of Applied Sciences, 8, 4434-4439.

Manzo, M., Ricciardi, G. P., Casu, F., Ventura, G., Zeni, G., Borgström, S., 2006. Surface deformation analysis in the Ischia island (Italy) based on spaceborne radar interferometry. J. Volcanol. Geotherm. Res., 151, 399−416.

Osmanoğlu, B., Dixon, T.H., Wdowinski, S., Cabral-Cano, E., Jiang, Y., 2011. Mexico City subsidence observed with persistent scatterer InSAR. Intern. J. Appl. Earth Observ. Geoinform., 13, 1-12, doi: 10.1016/j.jag.2010.05.009.

Orsi, G., De Vita, S., Di Vito, M., 1996. The Restless, Resurgent Campi Flegrei Nested Caldera (Italy): Constraints on its Evolution and Configuration. J. Volcanol. Geotherm. Res., 74, 179–214.

Pellegrino, A., 1967. Proprietà fisico-meccaniche dei terreni vulcanici del napoletano. Atti VIII Convegno di Geotecnica, Cagliari, 113-145.

Perrotta, A., Scarpati, C., Luongo, G., Morra, V., 2006. Chapter 5: The Campi Flegrei caldera boundary in the city of Naples, In: De Vivo, B., (Ed.), Developments in Volcanology. Elsevier, Amsterdam, 9 (C), 85-96, doi: 10.1016/S1871-644X(06)80019-7.

Piochi, M., Bruno, P.P., De Astis, G., 2005. Relative roles of rifting tectonics and magma ascent processes: Inferences from geophysical, structural, volcanological, and geochemical data for the Neapolitan volcanic region (southern Italy). Geochem. Geophys. Geosyst., 6, Q07005, doi:10.1029/2004GC000885.

Provincia di Napoli, Assessorato Miniere e Risorse Geotermiche (2004). Carta idrogeologica della Provincia di Napoli scala 1:50.000, Provincia di Napoli, Napoli.

Regione Campania (2005). Decreto del Presidente della Giunta regionale della Campania n° 323/11 giugno 2004. Boll. Uff. Reg. Campania, 9, 1-10.

Remy, D., Bonvalot, S., Murakami, M., Briole, P., Okuyama, S., 2006. Inflation of Aira Caldera (Japan) detected over Kokubu urban area using SAR interferometry ERS data. eEarth Discuss., 1, 151–165.

Sbrana, A., Giulivo, I., Monti, L., D'elia, G., Miraglino, P., Giordano, F., Isaia, R., Luperini, W., Perrotta, L., Scarpati, C., Toccaceli, R. Vietina, M., 2007. The geology of Napoli megacity in the framework of the new geological survey of Napoli sheet (CAR.G.

Project). Proc. 5th European Congress on Regional Geoscientific Cartography and Information Systems. Revista Catalana de Geografia, 12 (29). http://www.rcg.cat/articles.php?id=54

Scarpati, C., Perrotta, A., Lepore, S., Calvert, A., 2013. Eruptive history of Neapolitan volcanoes: constraints from 40Ar–39Ar dating. Geol. Magaz., 150, 412-425. doi:10.1017/S0016756812000854.

Scarpati, C., Cole, P., Perrotta, A., 1993. The Neapolitan Yellow Tuff - A Large Volume Multiphase Eruption from Campi Flegrei, Southern Italy. Bull. Volcanol. 55, 343–356.

Shepard, D., 1968. A two-dimensional interpolation function for irregularly-spaced data. Proceedings of the 1968 ACM National Conference, 517–524. doi:10.1145/800186.810616

Stramondo, S., Bozzano, F., Marra, F., Wegmuller, U., Cinti, F.R., Moro, M., Saroli, M., 2008. Subsidence induced by urbanization in the city of Rome detected by advanced InSAR technique and geotechnical investigations. Rem. Sens. Environ., 112, 3160–3172.

Stumpf, A.J., 2013, Hydrocompaction subsidence. In: Bobrowsky P.T. (ed.), Encyclopedia of Natural Hazards. Springer Netherlands, 496-497, doi: 10.1007/978-1-4020-4399-4_177

Tangenziale Di Napoli, 2001. Indagini geognostiche e geotecniche relative alla ricostruzione e all'ampliamento della stazione della zona ospedaliera, Relazione Geologico Tecnica. Documento interno TANGENZIALE DI NAPOLI S.P.A.

Terranova, C. , Vilardo, G., Isaia, R., Iannuzzi, E., Pignataro, F., 2012. Telerilevamento e classificazione delle subsidenze nell'area metropolitana di Napoli tramite interpretazione di dati interferometrici radar PS. Riv. Quadri. Ord. Naz. Geologi, Roma, Marzo 2012 1/12, ISSN 1722-0025.

Terranova, C., Iuliano, S., Matano, F., Nardò, S., Piscitelli, E., Cascone, E., D'Argenio, F., Gelli, L., Alfinito, M., Luongo, G., 2009. The TELLUS Project: a satellite-based slow-moving landslides monitoring system in the urban areas of Campania Region. Rend. Soc. Geol. It., 8, 148-151.

Tesauro, M., Berardino, P., Lanari, R., Sansosti, E., Fornaro, G., Franceschetti, G., 2000. Urban Subsidence inside the city of Napoli (Italy) observed by satellite radar interferometry. Geophys. Res. Lett., 27 (13), 1961-1964.

Vallario, A., 1992. Sprofondamenti e crolli nelle cavità del sottosuolo napoletano. In: Frane e territorio, Liguori Editori, Napoli, 427-458.

Ventura G., Vilardo G., Terranova C., Bellucci Sessa E. (2011) Tracking and evolution of complex active landslides by multi-temporal airborne LiDAR data: the Montaguto landslide (Southern Italy). Rem. Sens. Env., 115, 3237-3248, doi:10.1016/j.rse.2011.07.007

Vilardo, G., Isaia, R., Ventura, G., De Martino, P., Terranova, C., 2010. InSAR Permanent Scatterer analysis reveals fault reactivation during inflation and deflation episodes at Campi Flegrei caldera. Rem. Sens. Env., 114, 2373-2383.

Vilardo, G., Ventura, G., Terranova, C., Matano, F., Nardò, S., 2009. Ground deformation due to tectonic, hydrothermal, gravity, hydrogeological, and anthropic processes in the Campania Region (Southern Italy) from Permanent Scatterers Synthetic Aperture Radar Interferometry. Rem. Sens. Env., 113, 197–212.

Vitale, S., Isaia, R., 2014. Fractures and faults in volcanic rocks (Campi Flegrei, southern Italy): insight into volcano‐tectonic processes. Int. J. Earth Sci., 103, 801–819, doi: 10.1007/s00531-013-0979-0

Wang, Z., Perissin, D., Lin, H., 2011. Subway tunnels identification through Cosmo-SkyMed PSInSAR analysis in Shanghai. Geoscience and Remote Sensing Symposium IGARSS, Vancouver, 1267 – 1270, doi: 10.1109/IGARSS.2011.6049430

Yan, D., Ge, D., Yang, J., Zhang, L., Wang, Y., Guo, X., 2010. PSI analyses of land subsidence due to economic development near the city of Hangzhou, China. Proc. IGARSS 2010, 2410-2413.

Zhang, Y., Zhang, J., Wu, H., Lu, Z., Guangtong, S., 2011. Monitoring of urban subsidence with SAR interferometric point target analysis: A case study in Suzhou, China. Intern. J. Appl. Earth Observ. Geoinform, 13, 812–818 doi:10.1016/j.jag.2011.05.003

Figure Captions

Figure 1 - (a) Location of Napoli city, Campi Flegrei caldera and Somma-Vesuvius volcano; the black polygon is the administrative boundary of the Napoli municipality; the red lines define the Campi Flegrei caldera rims (data from Perrotta et al. (2006), Scarpati et al. (2013) and Vitale and Isaia (2014)). (b) Lithological sketch map of Napoli (modified from Comune di Napoli, 1999) with isopiezometric contour lines (in m above the sea level, blue dashed

lines) and main drainage axes (arrows) (modified from Celico et al., 2001); the three main hydrological sectors of the Napoli are also reported. The dotted line A-B in represents the trace of the profile in Fig. 5. Symbols: 1 Alluvial, beach and marine deposits, and landfill material, 2 Mainly unlithified and cohesionless pyroclastics younger than 15 ka of the Campi Flegrei activity, 3 lithified to unlithified Neapolitan Yellow Tuff deposits (15 ka) and unlithified pyroclastics with age between 15 and 39 ka, 4 Campanian Ignimbrite (CI) lithified tuffs and loose pumice lapilli and ash layers (39 ka), and older lithified to unlithified tuffs of the Napoli city volcanoes (up to 80 ka), 5 pyroclastic deposits of the Somma-Vesuvius historical activity, 6 pyroclastic deposits of the Somma-Vesuvius pre-historical activity, 7 Anthropic cavities and underground cavities of the Napoli metropolitan area.

Figure 2 - Map view of the PS (coherence>0.65) range-change rate measurements computed from: (a) ascending, and (b) descending ERS data (1992 - 1999), and (c) ascending and (d) descending Radarsat (2003 - 2007). Positive values indicate a decrease in the range (distance from the satellite to point on the ground). The insets show the satellite flight direction (black arrow) and the look direction (red arrow); the number (degree) refers to the incidence angle (data from Vilardo et al. (2010).

Figure 3 - Mean deformation velocities estimated using SAR data. (a) and (b) show the vertical and East–West components of the average deformation velocity generated from ERS data, respectively. (c) and (d) report, respectively, the vertical and East–West components of the average deformation velocity generated from Radarsat data. The abbreviations refer to the main subsiding areas discussed in the text: VA (Vomero-Arenella district), SS (Scudillo-

Stella district), MS (Municipio Square), GS (Garibaldi Square), PD (Poggiorele district). Gray areas have deformation velocity = 0.0±0.5 mm/yr, as specified in the legend.

Figure 4 - Vomero-Arenella district (VA in Fig. 3): vertical component of the average deformation velocity generated from ERS (a) and Radarsat (b) data. The location of PS from ascending (square) and descending (circle) acquisition geometries is also reported in (a) and (b). In the background, the digital color orthophoto (2011). The CI caldera faults are reported as red lines with triangle (location from Perrotta et al. (2006)). (c) LOS mean deformation time series for ERS (1992-2001) and Radarsat (2003-2007) PS with the maximum deformation rate in the Vomero-Arenella district. RS= Radarsat, A= ascending, B= descending. Negative values indicate movement away from the satellite along LOS.

Figure 5 - Profile along the Vomero-Arenella district reporting the topography (black), the vertical components of the velocity from ERS (red) and Radarsat (blue) data, and the faults of Fig. 4. The trace of the profile is in Fig. 1b. The CI caldera faults are reported as red dashed lines (from Perrotta et al., 2006).

Figure 6 - Scudillo-Stella district (SS in Fig. 3): vertical component of the average deformation velocity generated from ERS (a) and Radarsat (b) data. The location of PS from ascending (square) and descending (circle) acquisition geometries is also reported in (a) and (b). The black polygon represents the projection on the surface of the underground water reservoir. The trace of the SW–NE and SE-NW profiles depicted in Fig. 8 is also reported in (a). Color scale as in Fig. 4b. In the background, a digital color orthophoto acquired in 2011.

The inset right of (b) reports the results of a structural survey carried out by us in the galleries surrounding the underground reservoir and shows the stereographic projection of the recorded fractures (Schmidt net, lower projection); the red plane represents the best fitting plane (dip direction 224°; dip 55°) of the NW-SE striking fractures. (c) LOS mean deformation time series for ERS (1992-2001) and Radarsat (2003-2007) PS with the maximum deformation rate in the Scudillo-Stella district. RS= Radarsat, A= ascending, B= descending. Negative values indicate movement away from the satellite along LOS.

Figure 7 - (a) Location of the available wells (yellow dots) around the Scudillo-Stella district (SS in Fig. 3). The water reservoir is also reported; (b) Stratigraphy from the well logs (data from Comune di Napoli, (1999), and Tangenziale di Napoli (2001).

Figure 8 - NW-SE and SW-NE profiles across the Scudillo-Stella district reporting the topography (black), the vertical components of the velocity from ERS (red) data, the top of the NYT deposits (blue dots), and the location of the underground water reservoir is also reported. The trace of the profiles is in Fig. 6a.

Figure 9 - Municipio square (MS in Fig. 3). Vertical component of the average deformation velocity generated from ERS (a) and Radarsat (b) data. Color scale as in Fig. 4b. The location of PS from ascending (square) and descending (circle) acquisition geometries is also reported in (a) and (b). The PS selected for the LOS mean deformation time series reported in Fig. 11 are within the main subsiding area enclosed by the dashed line. The background in (a) and (b) are digital color orthophotos acquired in 1998 and 2011, respectively. The route of the

subway tunnel (black line) and the excavation area of the subway stations (blue box) are also reported.

Figure 10 - Garibaldi square (GS in Fig. 3). Vertical component of the average deformation velocity generated from ERS (a) and Radarsat (b) data. Color scale as in Fig. 4b. The location of PS from ascending (square) and descending (circle) acquisition geometries is also reported. The PS selected for the LOS mean deformation time series reported in Fig. 11 are within the main subsiding area enclosed by the dashed line. The background in (a) and (b) are digital color orthophotos acquired in 1998 and 2011, respectively. The subway tunnel (black line with tracks) and the excavation area of the subway stations (blue box) are also reported.

Figure 11 - LOS mean deformation time series for Radarsat PS located in Municipio (Fig. 9) and Garibaldi (Fig. 10) squares. Negative values indicate movement away from the satellite along LOS. The selected PS are those enclosed in the area of maximum subsidence bounded by the dashed line in Figs. 9 and 10.

Figure 12 - Poggioreale district (PD in Fig. 3). Vertical component of the average deformation velocity generated from ERS (a) and Radarsat (b) data. Color scale as in Fig. 4b. The location of PS from ascending (square) and descending (circle) acquisition geometries is also reported. In the background, a digital color orthophoto acquired in 2011. The banked railway lines (black line with tracks) and the elevated highway (thick white line) are also reported. (c) LOS mean deformation time series for ERS (1992-2001) and Radarsat (2003-2007) PS with the maximum deformation rate in the Poggioreale district. RS= Radarsat, A=

ascending, B= descending. Negative values indicate movement away from the satellite along LOS. The piezometric level variations with time are reported in blue (data from two wells located at a distance of 600 m northwest from the banked railway; Allocca and Celico, 2008; Corniello and Ducci, 2013). The average rates of the water table rise are also reported in m/yr. (d) Oedometer test results of neapolitan volcanic soil ‘pozzolana’ (data from Pellegrino, 1967). The bleu arrows mark the cycle of loading. Note the collapse of the sample at constant pressure when the water is added.

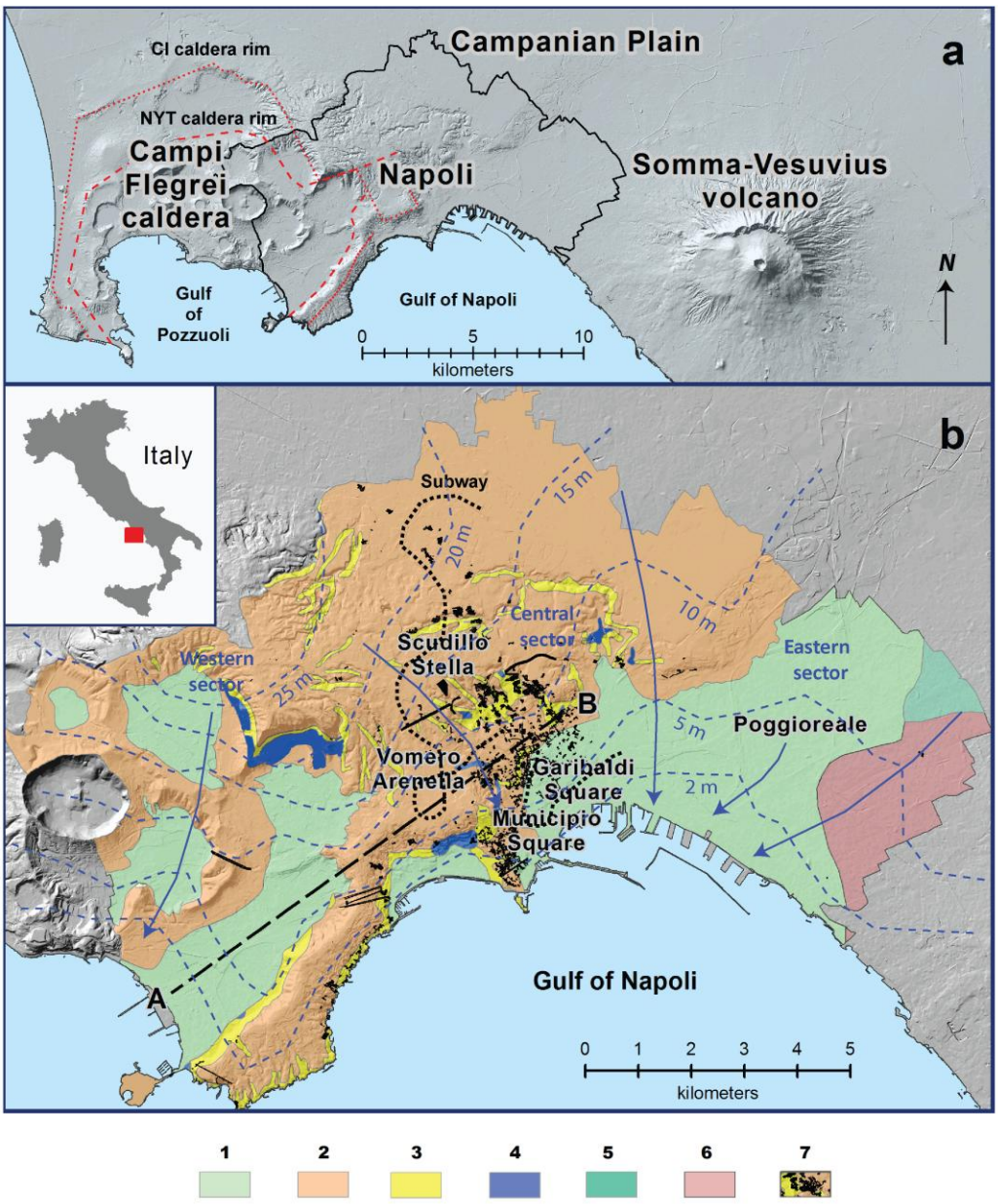

Figure 1

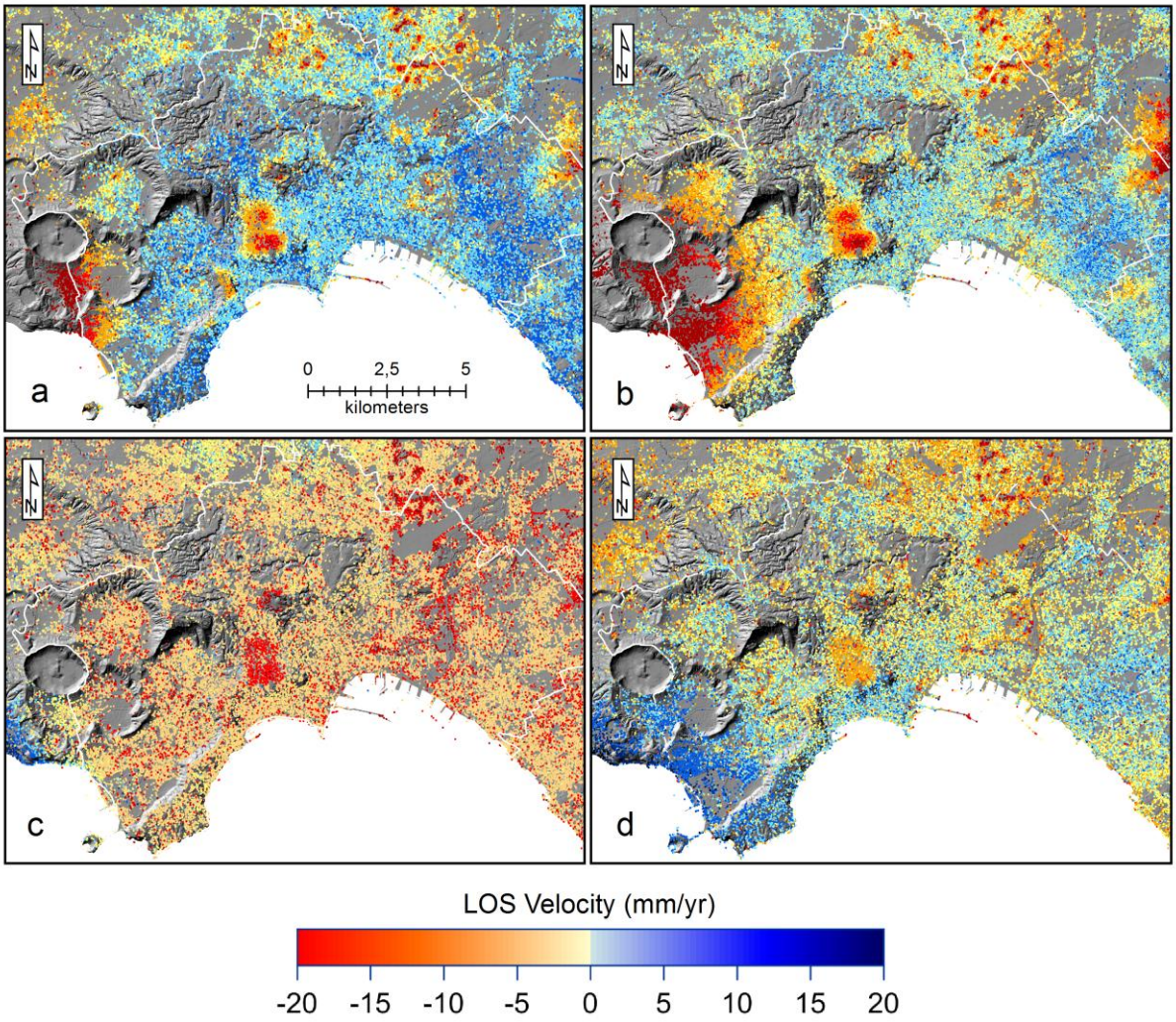

Figure 2

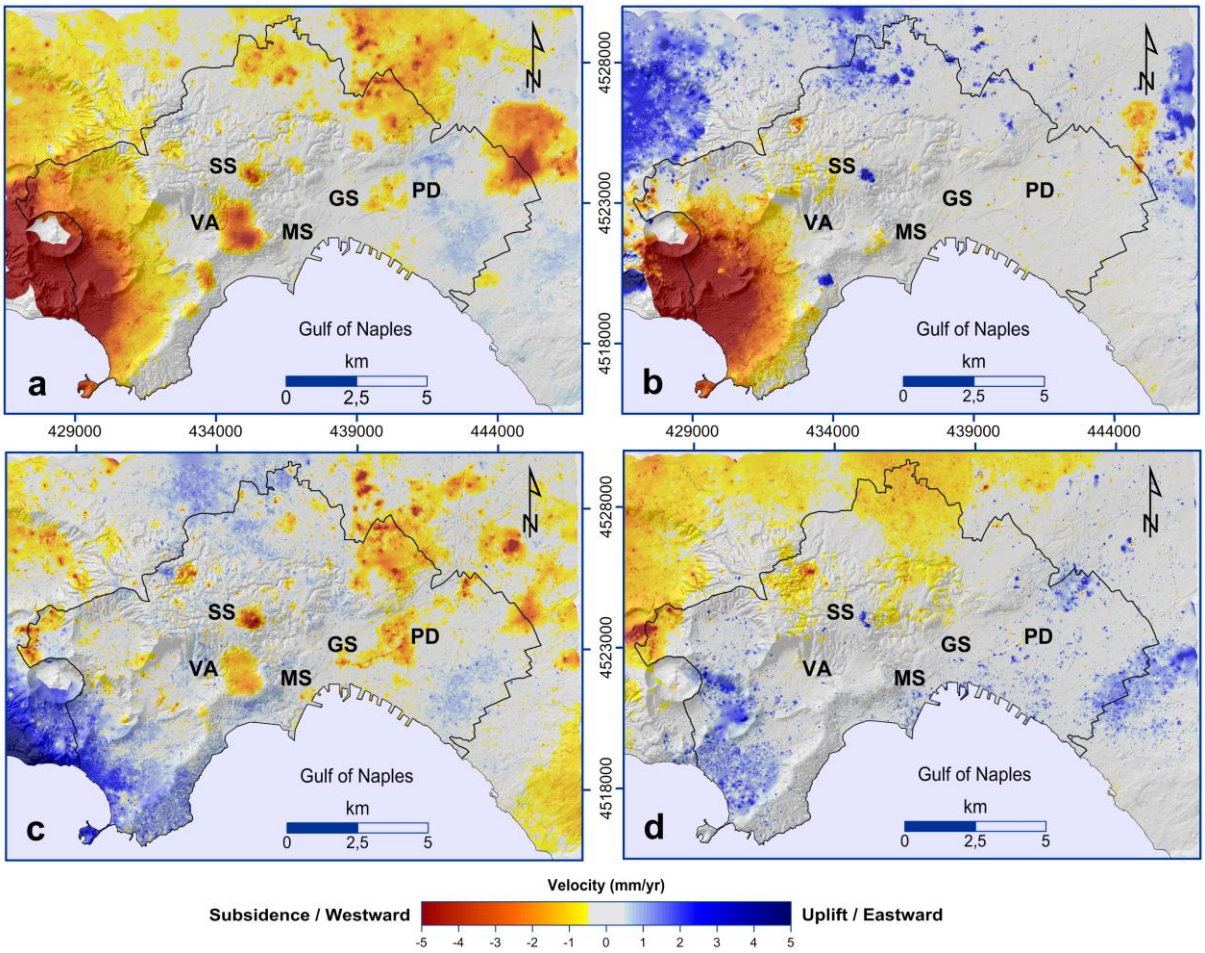

Figure 3

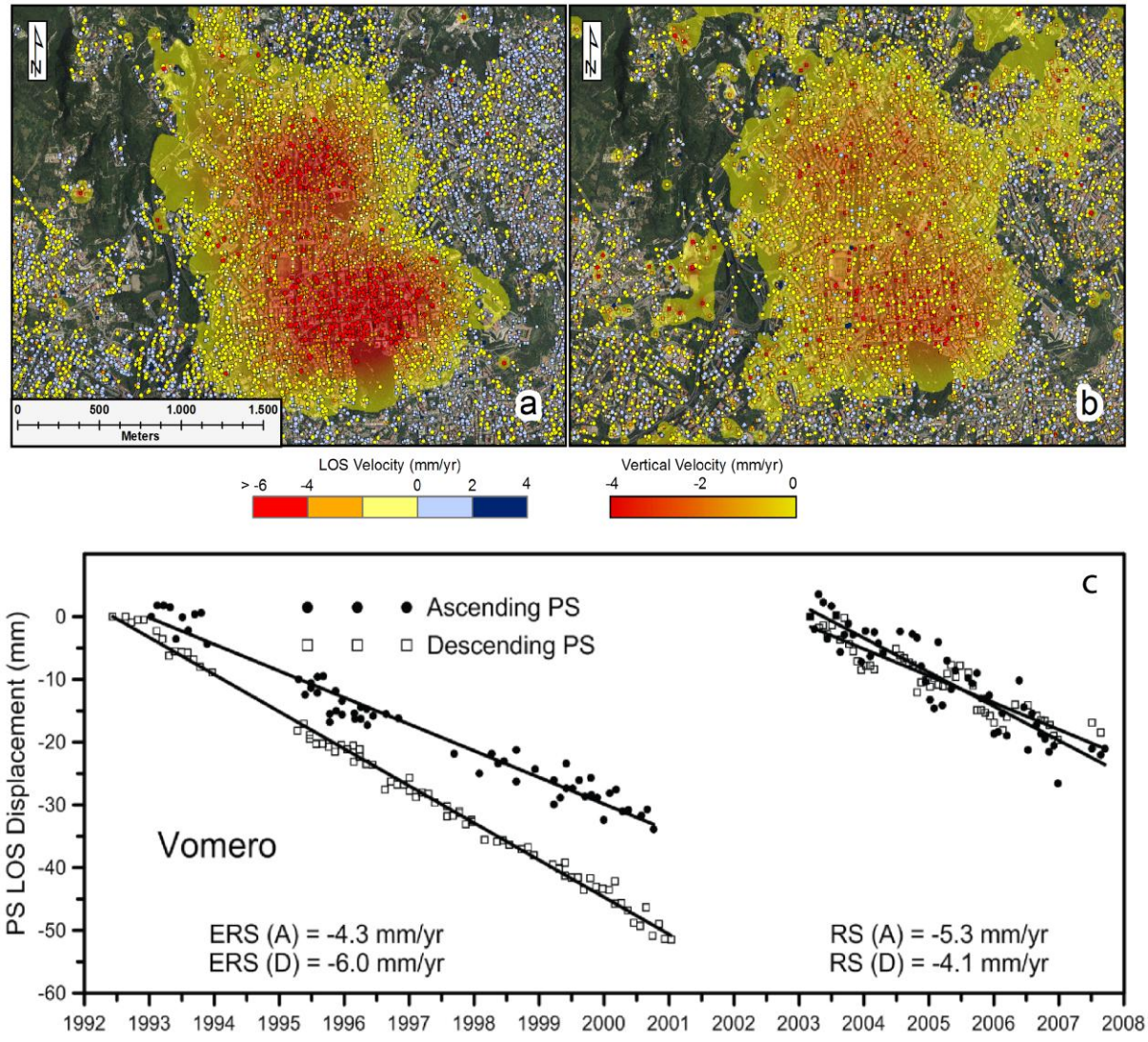

Figure 4

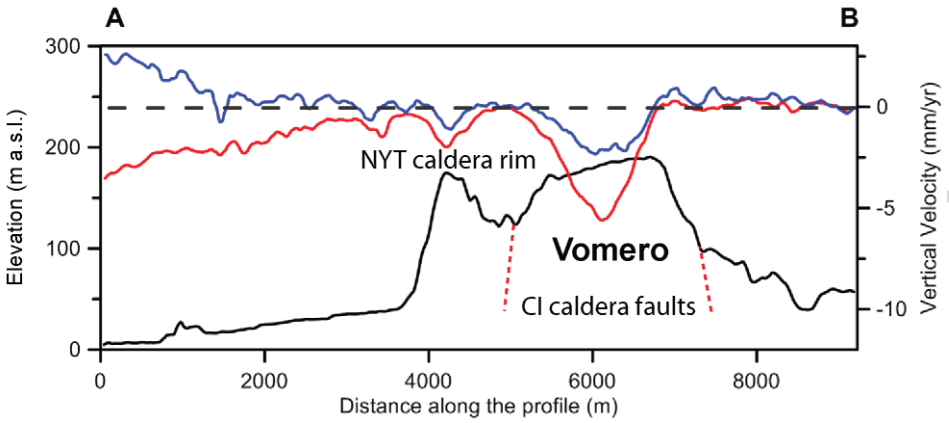

Figure 5

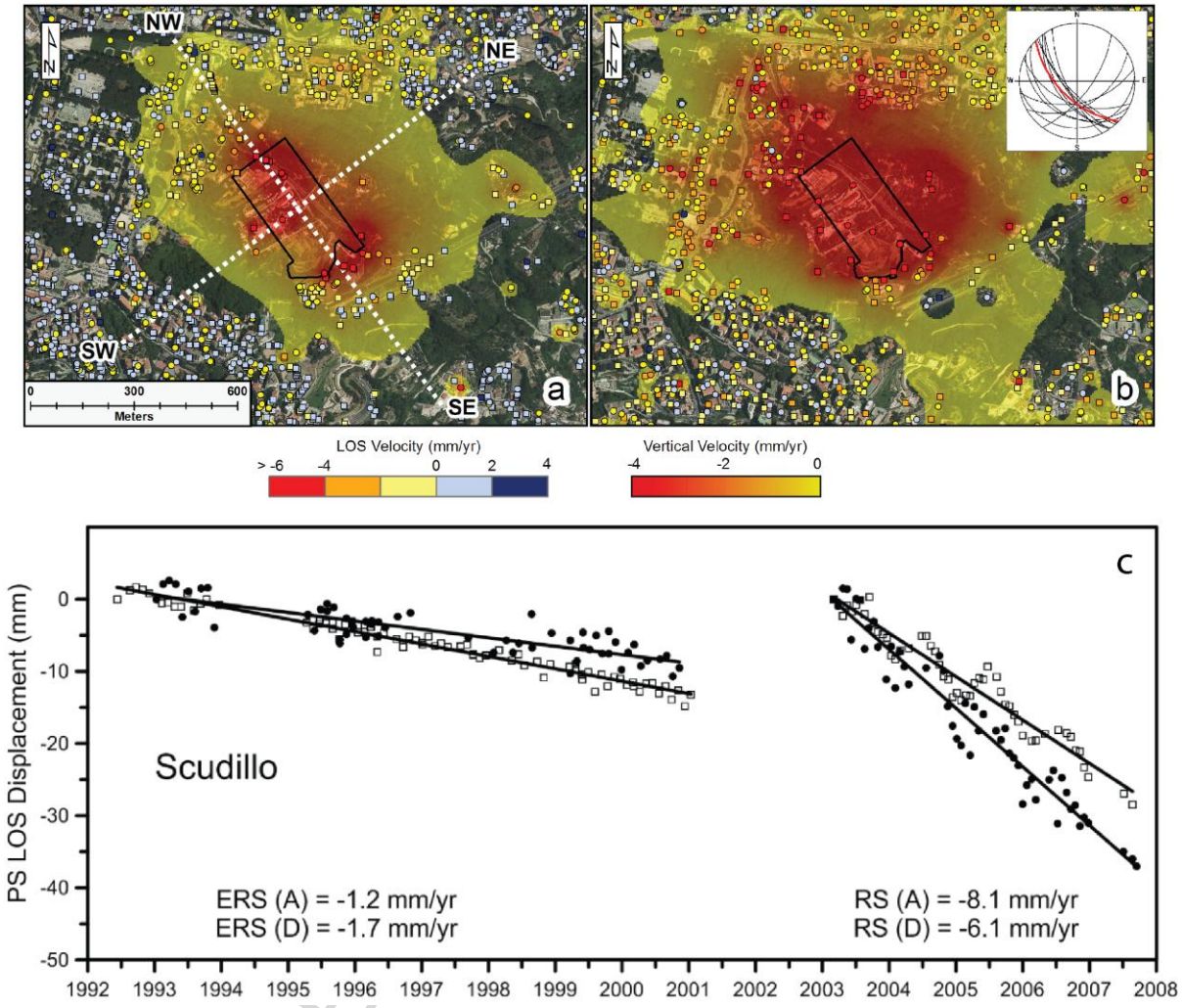

Figure 6

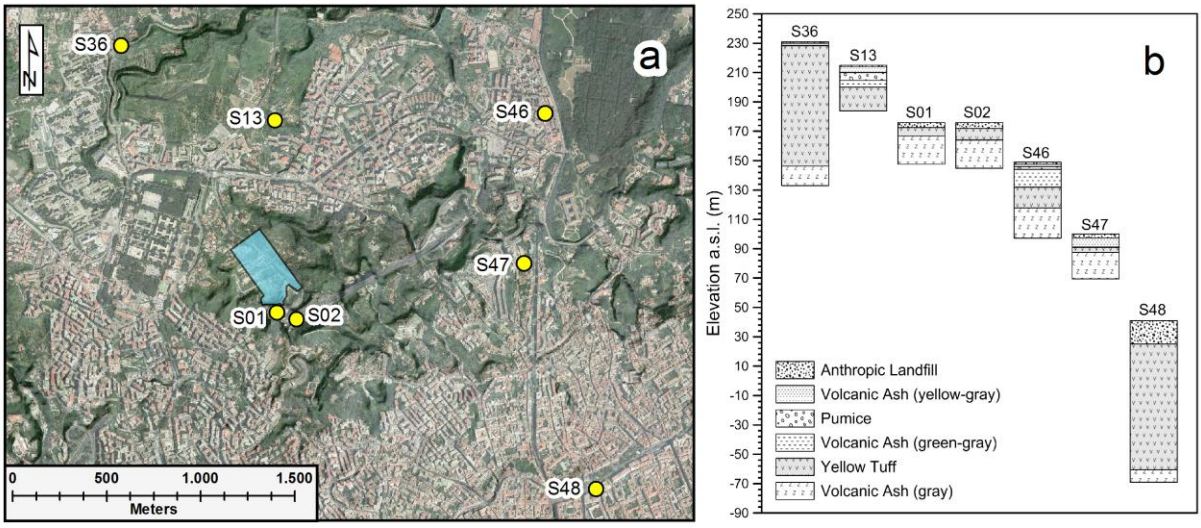

Figure 7

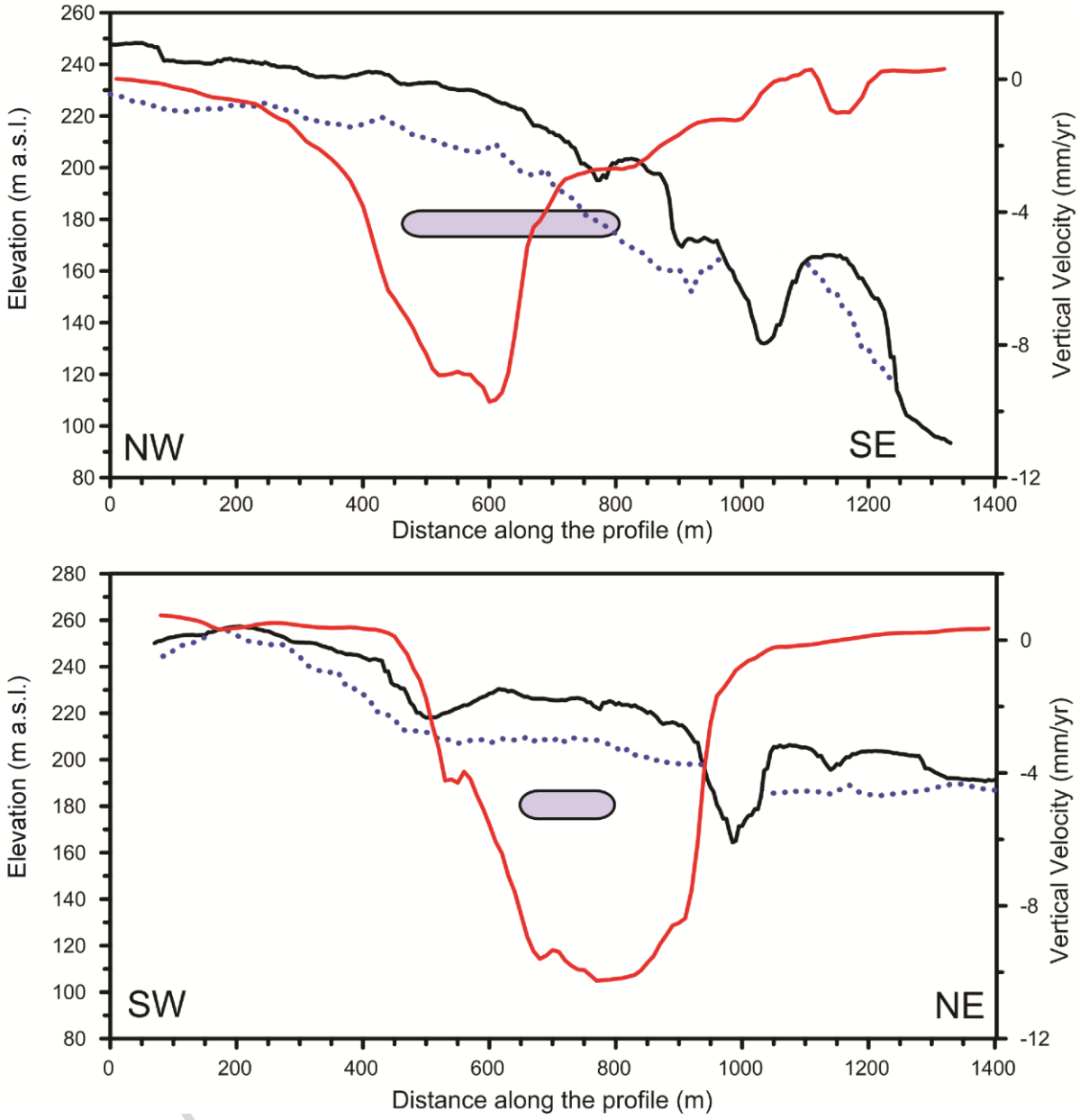

Figure 8

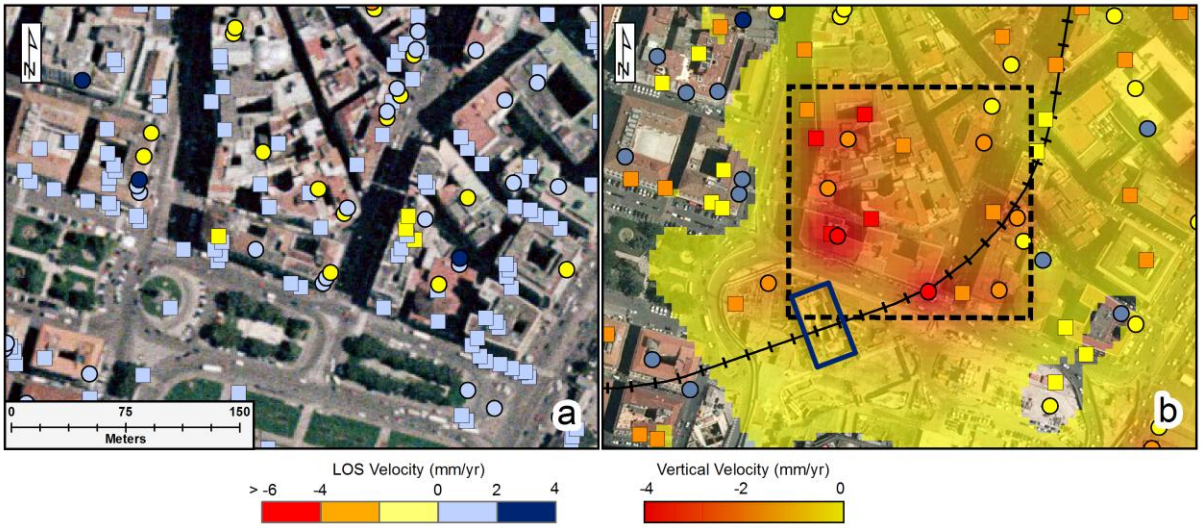

Figure 9

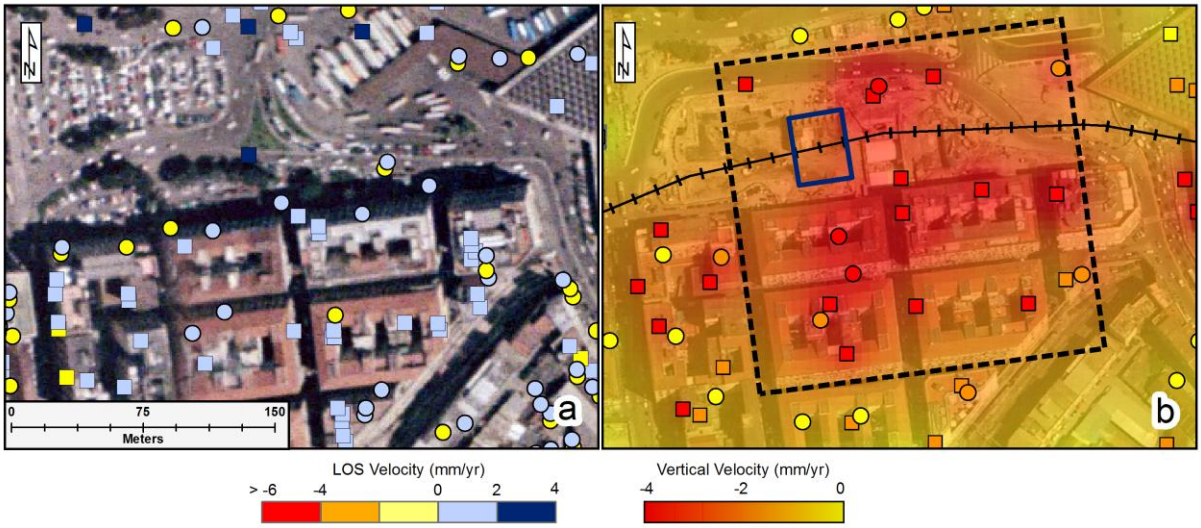

Figure 10

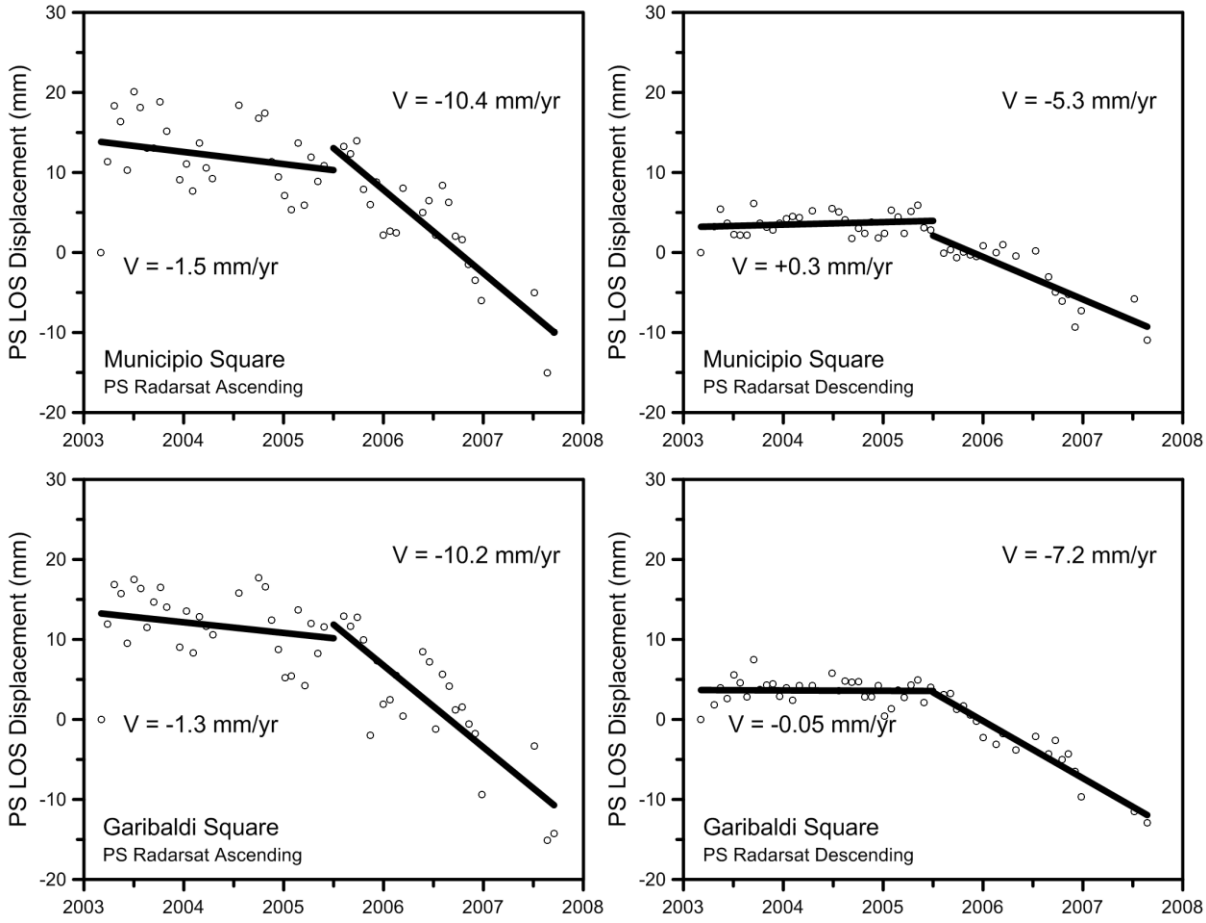

Figure 11

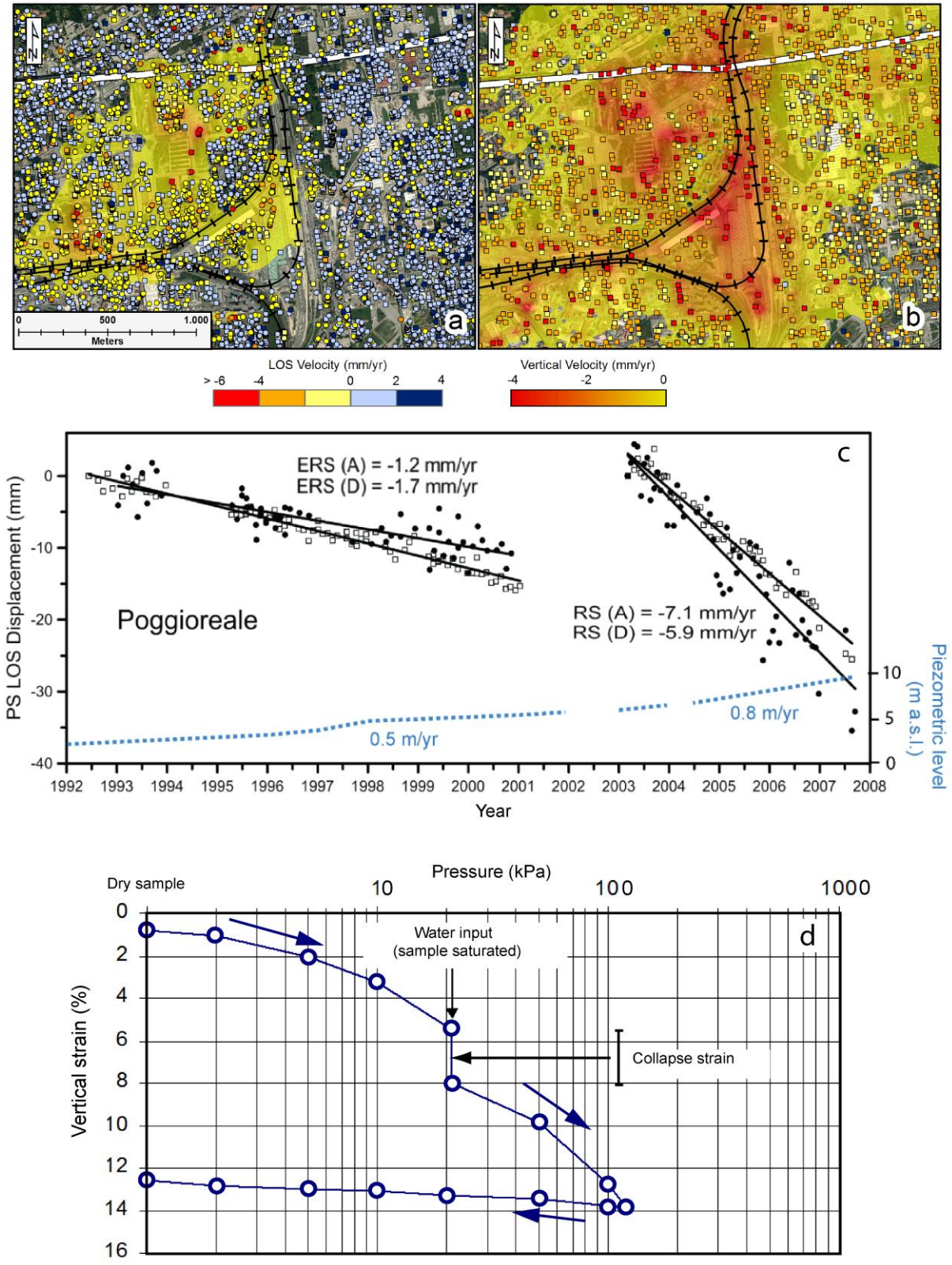

Figure 12

District/Quarter	Max deformation value (mm/year) 1992-2001 (ERS)	Max deformation value (mm/year) 2003-2007 (Radarsat)
Vomero-Arenella	-5.7	-5.6
Scudillo Stella	-1.6	-8.6
Municipio Square	-1.5	-9.5
Garibaldi Square	-1.3	-10.5
Poggioreale	-1.6	-7.8

Table 1. Maximum values of the vertical deformation velocity measured in the selected zones of the Napoli metropolitan area.